Quantitative Trait Loci for Inflorescence Development in *Arabidopsis thaliana*

Mark C. Ungerer, Solveig S. Halldorsdottir, Jennifer L. Modliszewski, Trudy F. C. Mackay and Michael D. Purugganan[1]

Department of Genetics, North Carolina State University, Raleigh, North Carolina 27695

Manuscript received August 13, 2001
Accepted for publication December 17, 2001

ABSTRACT

Variation in inflorescence development patterns is a central factor in the evolutionary ecology of plants. The genetic architectures of 13 traits associated with inflorescence developmental timing, architecture, rosette morphology, and fitness were investigated in *Arabidopsis thaliana*, a model plant system. There is substantial naturally occurring genetic variation for inflorescence development traits, with broad sense heritabilities computed from 21 Arabidopsis ecotypes ranging from 0.134 to 0.772. Genetic correlations are significant for most (64/78) pairs of traits, suggesting either pleiotropy or tight linkage among loci. Quantitative trait locus (QTL) mapping indicates 47 and 63 QTL for inflorescence developmental traits in L*er* × Col and Cvi × L*er* recombinant inbred mapping populations, respectively. Several QTL associated with different developmental traits map to the same Arabidopsis chromosomal regions, in agreement with the strong genetic correlations observed. Epistasis among QTL was observed only in the Cvi × L*er* population, and only between regions on chromosomes 1 and 5. Examination of the completed Arabidopsis genome sequence in three QTL regions revealed between 375 and 783 genes per region. Previously identified flowering time, inflorescence architecture, floral meristem identity, and hormone signaling genes represent some of the many candidate genes in these regions.

THE inflorescence is a central element of the shoot system of flowering plants (Coen and Nugent 1994; Tucker and Grimes 1999). Arrayed on inflorescence shoots are the flowers that serve as the main reproductive structures of angiosperm taxa. The development of the inflorescence, including the timing of ontogenetic events that lead to the morphological elaboration of mature inflorescence shoots, plays a crucial role in the ecology and evolution of flowering plant species (Coen and Nugent 1994; Fishbein and Venable 1996; Diggle 1999). Several life history characteristics are controlled by the timing of the transition from vegetative to reproductive development (Mitchell-Olds 1996; Kuittinen *et al.* 1997; Stratton 1998; Diggle 1999), while plant reproductive ecology is determined, in part, by the architecture of the inflorescence shoot (Schoen and Dubec 1990; Fishbein and Venable 1996; Diggle 1999). Inflorescence architectures display a wide range of diversity among plant species (Coen and Nugent 1994) and are critical determinants of interspecies differences in plant morphology and life history.

Diversity of inflorescence morphologies within and between species arises through the functions, fates, and positions of meristems distributed along the inflorescence shoot axis (Sussex and Kerk 2001). In the model plant *Arabidopsis thaliana*, the main inflorescence shoot is an elongated stem whose features develop from three types of reproductive meristems: the primary apical inflorescence meristem, secondary inflorescence meristems, and the floral primordia (Bowman 1994; Hempel and Feldmann 1994). The reproductive shoot apex contains the indeterminate, primary inflorescence meristem that produces the main inflorescence axis of the plant. At the flanks of the main inflorescence meristem, secondary inflorescence meristems and floral primordia are established (Hempel and Feldmann 1994). Secondary inflorescence meristems are positioned at basal nodes of the main inflorescence shoot and are subtended by bract-like cauline leaves. These secondary meristems develop into axillary inflorescences, sometimes referred to as coflorescences; axillary inflorescences can also emerge from the axils of basal rosette leaves. Floral meristems or primordia also develop closer to the apices of the main and axillary inflorescence shoots, and the total reproductive output of Arabidopsis plants results from floral meristem activity on all inflorescence shoots.

The precise details of Arabidopsis inflorescence architecture are characterized by the numbers and distribution of axillary inflorescence shoots and main axis flowers, which in turn are governed by the development and distribution of all three reproductive meristem types (Figure 1). The developmental phenotypes associated with inflorescence shoot development are generally manifested as quantitative traits that vary either continuously or meristically between individuals or genetic

[1]*Corresponding author:* Department of Genetics, Box 7614, North Carolina State University, Raleigh, NC 27695.
E-mail: michael_purugganan@ncsu.edu

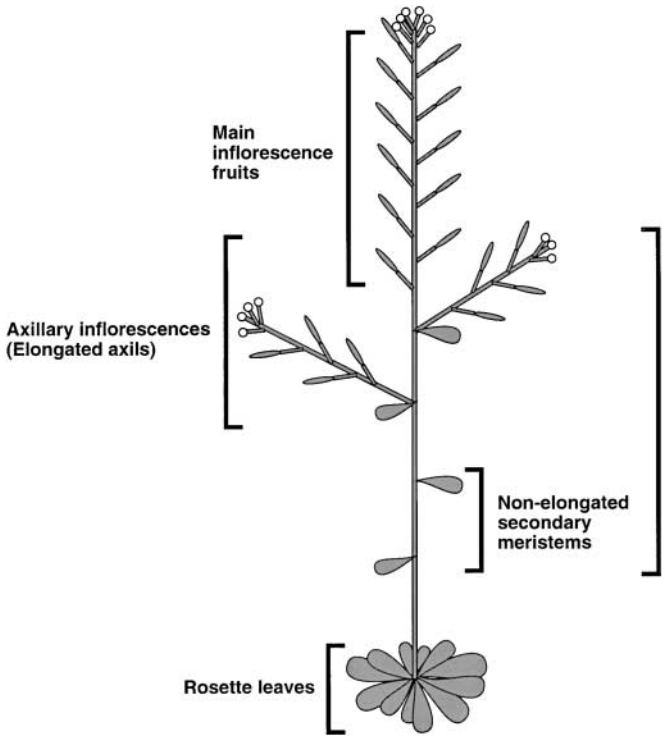

Figure 1.—Architecture of *A. thaliana*.

lines. Quantitative variation in Arabidopsis inflorescence morphology results in intraspecific architectural diversity, with some individuals possessing highly branched inflorescences with numerous axillary inflorescences, while others have reproductive architectures marked by only one main inflorescence shoot and no (or few) axillary inflorescences. Developmental decisions such as meristem allocation, fate, and timing (Sussex and Kerk 2001) are thus observed as quantitative variation in the number of main axis inflorescence meristems established, the number of elongated axillary inflorescences, or the timing of shoot bolting. Identification of genes that lead to variation in quantitative aspects of inflorescence morphology can thus provide insights into developmental pathways that lead to diversity in plant reproductive shoot architectures.

In the last few years, geneticists have managed to identify and isolate several Arabidopsis genes that regulate the development of the inflorescence (Shannon and Meeks-Wagner 1991, 1993; Bowman *et al.* 1993; Bradley *et al.* 1997; Koornneef *et al.* 1998a; Levy and Dean 1998; Schmitz and Theres 1999). Several of these loci are known, through mutant analysis, to control the timing of inflorescence development by regulating the transition of vegetative to inflorescence shoot development (Koornneef *et al.* 1998a; Levy and Dean 1998) and the sensitivity of this developmental transition to environmental cues (Simpson *et al.* 1999). These flowering-time genes include, among others, *FLOWERING LOCUS C* (*FLC*; Michaels and Amasino 1999; Sheldon *et al.* 1999), *FRIGIDA* (*FRI*; Clarke and Dean 1994; Johanson *et al.* 2000), *CONSTANS* (*CO*; Putterill *et al.* 1995; Suarez-Lopez *et al.* 2001), *CRYPTOCHROME2* (*CRY2*; Guo *et al.* 1998, 1999), and *LUMIDEPENDENS* (*LD*; Lee *et al.* 1994). Other genes have been identified whose mutant phenotypes affect the types, distribution, and elongation of meristems along the inflorescence shoot. These include floral meristem identity genes such as *LEAFY* (Weigel *et al.* 1992), *APETALA1* (*AP1*), and *CAULIFLOWER* (*CAL*) (Mandel *et al.* 1992; Bowman *et al.* 1993; Kempin *et al.* 1995), the inflorescence architecture gene *TERMINAL FLOWER1* (*TFL1*; Shannon and Meekswagner 1991, 1993; Bradley *et al.* 1997), and hormone biosynthesis and activity genes (Blazquez *et al.* 1998; Walker and Estelle 1998) such as *AUXIN RESISTANT1* and *3* (*AXR1* and *AXR3*; Lincoln *et al.* 1990; Leyser *et al.* 1993; Ouellet *et al.* 2001).

With the exception of flowering (or bolting) time (Kowalski *et al.* 1994; Lee *et al.* 1994; Clarke *et al.* 1995; Mitchell-Olds 1996; Sanda *et al.* 1997; Koornneef *et al.* 1998a,b), however, genetic dissection of inflorescence development has not been undertaken in an explicitly quantitative genetic framework. Quantitative genetic studies, including the use of quantitative trait locus (QTL) mapping techniques, provide an opportunity to investigate the underlying genetic mechanisms that regulate developmental programs in plant architecture (Juenger *et al.* 2000; Mackay 2001). Quantitative genetic analysis permits investigators to examine the functions of previously identified developmental regulatory genes in new phenotypic contexts. QTL mapping approaches are also some of the first steps in identifying naturally occurring allelic variation and can serve as a gene discovery tool (Alonso-Blanco and Koornneef

TABLE 1

***A. thaliana* ecotypes examined for quantitative genetic variation in inflorescence development and morphology**

ABRC stock number	Ecotype (abbreviation)	Origin
CS1092	Columbia (Col-0)	Derived from Columbia (Col-1)
CS20	Landsberg *erecta* (L*er*-0)	Derived from Landsberg (La-0)
CS6059	Kent	United Kingdom
CS6098	Bretagny Sur Orge	France
CS6627	Basel (Bs-1)	Switzerland
CS6632	Burghaun/Rhon (Bu-0)	Germany
CS6633	Burghaun/Rhon (Bu-2)	Germany
CS6665	Chisdra (Chi-1)	Russia
CS6669	Coimbra (Co-1)	Portugal
CS6675	Cape Verde Islands (Cvi-0)	Cape Verde Islands
CS6701	Estland (Est-1)	Russia
CS6725	Graz (Gr-3)	Austria
CS6743	Vranov u Brno (Jl-1)	Czech Republic
CS6779	Limburg (Li-8)	Germany
CS6782	Llagostera (Ll-1)	Spain
CS6788	Lezoux (Lz-0)	France
CS6835	Playa de Aro (Pla-1)	Spain
CS6841	Frankfurt-Praunheim (Pr-0)	Germany
CS6850	Rschew (Rsch-4)	Russia
CS6852	San Eleno (Se-0)	Spain
CS6857	San Feliu (Sf-2)	Spain

2000; Mackay 2001; Yano 2001) by facilitating the identification of new inflorescence development genes. The identification of naturally occurring allelic variation in genes not only contributes to a greater understanding of the developmental genetics of the inflorescence, but also allows us to explore the evolutionary and ecological implications of variation in these development patterns.

MATERIALS AND METHODS

Arabidopsis ecotypes and mapping populations: Twenty-one ecotypes of *A. thaliana* originally collected over a wide range of the species distribution (Table 1) were analyzed for quantitative genetic variation in inflorescence development and morphology. Between 13 and 15 replicate individuals per ecotype were analyzed. Seeds of these ecotypes were obtained from the Arabidopsis Biological Resource Center at Ohio State University.

Two sets of recombinant inbred (RI) lines were utilized for QTL mapping of inflorescence development and morphology traits. The first set (L*er* × Col, 97 lines) is derived from a cross between ecotypes Landsberg *erecta* and Columbia (Lister and Dean 1993) and the second set (Cvi × L*er*, 160 lines) is derived from a cross between ecotypes Cape Verde Islands and Landsberg *erecta* (Alonso-Blanco *et al.* 1998a). Alleles of the Landsberg *erecta* ecotype are segregating in both sets of lines used in these experiments. All lines were advanced to the F_8 generation, were extensively genotyped, and are available from the Arabidopsis Biological Resource Center. Residual heterozygosity for the L*er* × Col and Cvi × L*er* RI lines has been estimated at 0.42% (Lister and Dean 1993) and 0.71% (Alonso-Blanco *et al.* 1998a), respectively; these values are similar to, and slightly less than, the theoretical expectation of 0.78%.

Because individuals of the same RI line are genetically identical, more precise estimates of genotype values can be obtained if replicate individuals per line are measured; QTL mapping can then be performed on RI line means. A total of 15 individuals from each line (for both sets of RI lines) were measured for all traits. Because some plants were lost during the experiment and because some seeds failed to germinate, between 11 and 14 and between 12 and 14 replicate individuals were measured for 4 L*er* × Col RI lines and for 21 Cvi × L*er* RI lines, respectively.

Plant growing conditions: Seeds were imbibed and cold treated at 4° for 4 days to break dormancy and promote uniform germination. Plants were grown in flats consisting of 72 cells, with one plant in each cell. Individuals were assigned to flat/cell positions in a way that minimized the number of replicate individuals of the same ecotype/RI line on a single flat but randomly assigned individuals to cell positions. For the ecotypes, this planting strategy resulted in 3 or 4 individuals of the same ecotype per flat; for the mapping populations, this resulted in (at most) one RI line replicate per flat. Assignment of plants to cell positions within individual flats was randomized. Any flat and/or positional effects were therefore randomized across the ecotype and RI lines. All plants were grown under long-day conditions (14 hr of light at 20°:10 hr of dark at 18°) in a growth chamber at the North Carolina State University Phytotron Facility and subirrigated with deionized water at regular intervals.

Inflorescence development and morphology traits: Thirteen traits (Table 2) reflecting various aspects of inflorescence development and morphology were measured on all individuals. These traits are categorized below, although many could be placed in more than one category.

1. Developmental timing:
   i. Bolting time: number of days from the transfer of seeds to the growth chamber to the emergence of the reproductive shoot;
   ii. Length of reproductive phase of main axis: number of days from bolting to abscission of the last petal on the youngest flower of the main axis;

TABLE 2

Summary statistics for 13 inflorescence development and morphology traits in a sample of 21 *A. thaliana* ecotypes

Trait	$\bar{X} \pm$ (SD)	$[V_G]^a$	$[V_E]^b$	$[H^2]^c$	$[CV_G]^d$
Bolting time (days)	34.08 (16.26)	251.926****	74.265	0.772	38.47
Length of reproductive phase of main axis (days)	19.05 (3.06)	8.733****	12.617	0.409	13.81
Time to maturity of main axis (days)	53.13 (17.90)	310.563****	96.564	0.763	28.13
Rosette leaves at bolting	12.81 (3.77)	13.291****	6.278	0.679	24.25
Rosette diameter (cm)	1.47 (0.13)	0.012****	0.062	0.166	6.83
Plant height (cm)	11.23 (1.99)	3.677****	4.659	0.441	15.34
Main inflorescence fruits	10.28 (1.35)	1.369****	6.851	0.167	10.13
Axillary fruits	8.60 (2.31)	4.316****	15.209	0.221	22.73
Nonelongated 2° meristems	0.69 (0.44)	0.137****	0.887	0.134	44.19
Elongated axils	2.69 (0.71)	0.432****	1.078	0.286	23.34
2° inflorescence meristems on main axis	3.35 (0.59)	0.287****	0.826	0.258	14.73
Early flowers	3.31 (0.79)	0.551****	1.198	0.315	20.67
Total fruits	18.65 (3.29)	8.882****	27.625	0.243	14.65

[a] Among-ecotype variance component from ANOVA; tests whether genetic differences exist among ecotypes for specified traits: ****$P \leq 0.0001$.

[b] Residual variance component from ANOVA.

[c] Measure of total phenotypic variance attributable to genetic differences among ecotypes (broad sense heritability) calculated as $V_G/(V_G + V_E)$.

[d] Coefficient of genetic variation calculated as $(100 \times \sqrt{V_G})/\bar{X}$.

iii. Time to maturity of main axis: number of days from the transfer of seeds to growth chamber to abscission of the last petal on the youngest flower of the main axis (bolting time + length of reproductive phase of main axis).

2. Rosette morphology:
   iv. Rosette leaves at bolting: number of basal rosette leaves produced at bolting;
   v. Rosette diameter: diameter (in centimeters) of rosette at maturity of main axis.
3. Inflorescence architecture:
   vi. Plant height: height (in centimeters) of main axis at maturity;
   vii. Main inflorescence fruits: number of fruits (siliques) produced on the main axis;
   viii. Axillary fruits: number of fruits produced on axillary inflorescences (in the L*er* × Col lines, this trait was scored as the number of fruits and flowers produced on axillary inflorescences at the time of maturity of the main axis; in the Cvi × L*er* lines, it was scored simultaneously with total fruits);
   ix. Nonelongated secondary meristems: number of main stem cauline leaves without an associated elongated axillary inflorescence;
   x. Elongated axils: number of elongated axillary inflorescences along the main stem;
   xi. Secondary inflorescence meristems on main axis: number of secondary inflorescence meristems produced along main axis (nonelongated secondary meristems + elongated axils).
4. Reproductive fitness:
   xii. Early flowers: cumulative number of flowers produced 7 days after bolting;
   xiii. Total fruits: total number of fruits produced throughout life span of plant (main inflorescence fruits + axillary fruits).

Some of these traits are depicted in Figure 1.

Quantitative genetic analysis: For each trait, total phenotypic variance was partitioned into sources attributable to ecotype (genotype, *G*) and error using a random effects analysis of variance (ANOVA) according to the model $y = \mu + G +$ error. Components of variance were used to estimate broad sense heritability according to the formula $V_G/(V_G + V_E)$, where V_G is the among-ecotype variance component and V_E is the residual (error) variance component. Genetic correlations (r_G) were estimated as $cov_{12}/\sqrt{V_{G1}V_{G2}}$, where cov_{12} is the covariance of trait means and V_{G1} and V_{G2} are the among-ecotype variance components for those traits (Roberston 1959). Confidence intervals (95%) for genetic correlation estimates were determined using a *z*-transformation (Sokal and Rohlf 1995). The coefficient of genetic variation (CV_G) was estimated for each trait as $(100 \times \sqrt{V_G})/\bar{X}$, where V_G is the among-ecotype variance component and $\bar{X}$ is the trait mean of the ecotypes (Houle 1992). Quantitative genetic analyses were conducted on RI lines in similar fashion to the ecotypes with the exception that among-line (instead of among-ecotype) variance components were determined and used in all statistical calculations. Analyses were conducted using statistical software packages SAS (GLM and VARCOMP procedures; SAS Institute 1988) and/or STATVIEW (SAS Institute 1999).

Linkage map construction: Genotype data for these lines are publicly available and were obtained on the web at http://nasc.nott.ac.uk/. Because not all lines have been genotyped for all markers and because the quality of a genetic map relies heavily on the accuracy and amount of genotype data in the mapping population, the maps used for QTL analyses were constructed from a subset of the total genotype data available. Markers were selected using the criteria that they be genotyped in ≥80% of lines and that they be distributed evenly throughout the genome. The L*er* × Col and Cvi × L*er* RI lines have been genotyped for largely different sets of markers. However, a small number of markers were mapped in both sets. These "integrating" markers were included in our data sets even if they were genotyped in <80% of lines.

Maps were constructed using Mapmaker/EXP 3.0 (Lander *et al.* 1987). Three-point likelihoods were computed (LOD > 3.0) for each linkage group prior to marker order determination with multipoint analysis. Marker orders were confirmed

by permuting positions of neighboring markers within a scrolling window (window size, five markers; log-likelihood threshold, 2.0) and comparing likelihoods of the permuted and original marker orders. Recombination frequencies were converted to centimorgan distances with the Kosambi (1944) mapping function.

QTL analyses: QTL for inflorescence development and morphology were mapped using the composite interval mapping (CIM; Zeng 1993, 1994) function of QTL Cartographer 1.13 (Basten *et al.* 1994, 1999). This procedure tests sequentially along each chromosome whether intervals flanked by two molecular markers contain a QTL while statistically accounting for other QTL segregating outside the tested interval. The identity (and number) of markers for this genetic background control was determined independently for each trait by forward selection, backward elimination stepwise regression. A 10-cM scan window was used for all analyses and the likelihood ratio (LR) test statistic, $2 \ln(L_0/L_1)$ [where L_0/L_1 is the ratio of likelihoods of two hypotheses, there is *no* QTL in the tested interval (L_0) and there *is* a QTL in the tested interval (L_1)] was calculated every 0.1 cM.

Experiment-wide significance thresholds for QTL identification were determined separately for each trait by permutation analysis (Churchill and Doerge 1994; Doerge and Churchill 1996). This procedure randomly permutes trait data and recalculates LRs across all genetic intervals. The most extreme LR value from each permutation is saved and used to generate a distribution of LRs to which empirical data are then compared. Empirical values equal to or exceeding the 5% highest values in the distribution of extreme permutation values are considered significant at $P < 0.05$. One thousand permutations were performed for each trait.

Tests for epistasis among QTL were conducted using ANOVAs to examine interaction effects of QTL with known additive effects (Long *et al.* 1995; Leips and Mackay 2000). For each test of epistasis involving pairwise combinations of QTL, an ANOVA model was fitted with main effects, including the markers nearest each QTL peak (as determined from QTL Cartographer) and a single interaction effect of two of these markers. A significant interaction effect in the analysis was interpreted as evidence for epistasis between QTL. Additional tests were performed until all pairwise combinations of markers were examined for each trait. Significance thresholds were adjusted using a sequential Bonferroni procedure. For each three-way test of epistasis, a model was fitted with main effects, including markers nearest each significant QTL peak, all significant two-way interactions, and a single three-way interaction. These analyses were conducted using the GLM procedure of SAS (SAS Institute 1988).

Candidate gene scan: Markers defining the limits of QTL regions (nearest and outside of the flanking 2-LOD support limits) were identified on the L*er* × Col genetic map and their positions on the Arabidopsis physical map were determined. The annotated sequence within these regions was then scanned for information regarding candidate genes (Arabidopsis Genome Initiative 2000). Because these regions represent large stretches of chromosomes (up to ~3.6 Mb), a computer program (written by M. C. Ungerer) was employed to scan the annotated sequence and provide summary information on candidate genes. Markers used to construct the Cvi × L*er* map have not been located on the Arabidopsis physical map and it was not possible to conduct a similar analysis for QTL mapped in the Cvi × L*er* RI lines.

RESULTS

Quantitative genetic variation for inflorescence development in *A. thaliana*: For all traits, among-ecotype variance was highly significant by ANOVA ($P \leq 0.0001$ in all instances), indicating substantial standing genetic variation for inflorescence developmental patterns in this species. Broad sense heritability estimates for these traits ranged from 0.134 (nonelongated secondary meristems) to 0.772 (bolting time) and averaged 0.373 (Table 2). These heritability estimates are, on average, lower than heritability estimates for floral morphology traits in *A. thaliana*, which ranged from 0.40 to 0.80 and averaged 0.67 (Juenger *et al.* 2000). Heritability estimates tended to be higher than average, however, for traits associated with developmental timing such as bolting time, length of reproductive phase, and time to maturity of main axis (mean heritability of 0.648 for developmental timing traits *vs.* mean heritability of 0.291 for all others).

There were significant genetic correlations among most traits (Table 3). These correlations ranged from −0.68 to the theoretical maximum of 1.0. Correlations with 95% confidence intervals *not* encompassing zero are considered significant; by this criterion, 82% of correlations were significantly different from zero. In addition, higher-order combinations of traits forming correlated blocks were identified. For example, bolting time, number of rosette leaves at bolting, and time to maturity of main axis were positively genetically correlated at ≥0.92. Bolting time and rosette leaves at bolting previously have been identified as strongly correlated in *A. thaliana* (Napp-Zinn 1969, 1985) but the strong correlation of these traits with time to maturity of main axis, to our knowledge, has not been previously observed. These strong genetic correlations suggest considerable developmental integration in these ecotypes and indicate that many pairwise and higher-order combinations of traits are likely influenced by the same loci (pleiotropy) or by tightly linked loci.

Quantitative variation was also explored in two sets of RI lines used for QTL mapping. Significant among-line variance was found for all traits in both sets of RI lines by ANOVA ($P < 0.01$ in all instances; Table 4). Broad sense heritability estimates for the L*er* × Col RI lines ranged from 0.034 (axillary fruits) to 0.522 (plant height) and averaged 0.215. For the Cvi × L*er* RI lines these estimates ranged from 0.129 (rosette diameter) to 0.744 (bolting time) and averaged 0.368. Similar to the ecotypes, heritabilities for developmental timing traits were higher than average in each set of RI lines.

Genetic correlations in the L*er* × Col and Cvi × L*er* RI lines are listed in Table 5. Genetic correlations ranged from −0.80 to 1.0 and from −0.71 to 1.0 for the L*er* × Col and Cvi × L*er* RI lines, respectively. Approximately 78 and 73% of these correlations were significantly different from zero for the L*er* × Col and Cvi × L*er* RI lines, respectively. Comparisons of the same correlations across the two sets of RI lines revealed that approximately two-thirds had overlapping 95% confidence intervals, indicating that many of the same traits were correlated in both the L*er* × Col and Cvi × L*er* RI

TABLE 3

Genetic correlations among inflorescence development and morphology traits in a sample of 21 *A. thaliana* ecotypes

	Total fruits	Early flowers	2° inflorescence meristems on main axis	Elongated axils	Nonelongated 2° meristems	Axillary fruits	Main inflorescence fruits	Plant height	Rosette diameter	Rosette leaves at bolting	Time to maturity of main axis	Length of reproduction phase of main axis
Bolting time	*−0.35* (*−0.52*, *−0.16*)	*−0.45* (*−0.60*, *−0.28*)	*−0.44* (*−0.59*, *−0.27*)	*−0.62* (*−0.73*, *−0.48*)	*0.40* (*0.22*, *0.56*)	*−0.51* (*−0.64*, *−0.34*)	−0.11 (−0.30, 0.09)	0.20 (0, 0.38)	*0.38* (*0.20*, *0.54*)	*0.94* (*0.91*, *0.96*)	*1.03*	*0.50* (*0.33*, *0.63*)
Length of reproductive phase of main axis	*0.22* (*0.02*, *0.40*)	*−0.68* (*−0.77*, *−0.55*)	−0.09 (−0.28, 0.11)	*−0.26* (*−0.43*, *−0.06*)	*0.23* (*0.04*, *0.41*)	0.09 (−0.11, 0.28)	*0.23* (*0.03*, *0.41*)	*0.51* (*0.34*, *0.64*)	*0.28* (*0.08*, *0.45*)	*0.44* (*0.27*, *0.59*)	*0.63* (*0.49*, *0.74*)	
Time to maturity of main axis	*−0.28* (*−0.45*, *−0.09*)	*−0.52* (*−0.65*, *−0.36*)	*−0.42* (*−0.57*, *−0.24*)	*−0.60* (*−0.71*, *−0.45*)	*0.40* (*0.22*, *0.55*)	*−0.44* (*−0.59*, *−0.26*)	−0.06 (−0.26, 0.14)	*0.26* (*0.07*, *0.44*)	*0.39* (*0.21*, *0.55*)	*0.92* (*0.88*, *0.94*)		
Rosette leaves at bolting	*−0.31* (*−0.48*, *−0.12*)	*−0.29* (*−0.47*, *−0.10*)	*−0.32* (*−0.49*, *−0.13*)	*−0.52* (*−0.65*, *−0.35*)	*0.44* (*0.26*, *0.59*)	*−0.50* (*−0.63*, *−0.33*)	0.03 (−0.17, 0.23)	*0.38* (*0.20*, *0.54*)	*0.49* (*0.33*, *0.63*)			
Rosette diameter	*−0.31* (*−0.48*, *−0.11*)	*−0.46* (*−0.61*, *−0.29*)	*−0.45* (*−0.60*, *−0.28*)	−0.15 (−0.34, 0.05)	*−0.46* (*−0.61*, *−0.29*)	*−0.36* (*−0.52*, *−0.17*)	*−0.35* (*−0.51*, *−0.16*)	*0.42* (*0.24*, *0.57*)				
Plant height	*0.23* (*0.03*, *0.41*)	*−0.34* (*−0.51*, *−0.15*)	0.15 (−0.05, 0.34)	0.16 (−0.04, 0.34)	−0.10 (−0.29, 0.10)	0.08 (−0.12, 0.28)	*0.31* (*0.12*, *0.48*)					
Main inflorescence fruits	*1.07*	*0.60* (*0.46*, *0.72*)	*0.39* (*0.21*, *0.55*)	*0.30* (*0.11*, *0.47*)	−0.02 (−0.21, 0.18)	*0.75* (*0.64*, *0.82*)						
Axillary fruits	*1.13*	*0.46* (*0.28*, *0.60*)	*0.55* (*0.40*, *0.68*)	*0.75* (*0.65*, *0.83*)	*−0.50* (*−0.64*, *−0.33*)							
Nonelongated 2° meristems	*−0.45* (*−0.59*, *−0.27*)	−0.03 (−0.23, 0.17)	0.08 (−0.12, 0.28)	*−0.66* (*−0.76*, *−0.53*)								
Elongated axils	*0.64* (*0.51*, *0.75*)	*0.26* (*0.07*, *0.44*)	*0.98* (*0.97*, *0.99*)									
2° inflorescence meristems on main axis	*0.50* (*0.34*, *0.64*)	*0.27* (*0.08*, *0.45*)										
Early flowers	*0.49* (*0.33*, *0.63*)											

Genetic correlations (r_G) were calculated as $\mathrm{cov}_{12}/\sqrt{V_{G1}V_{G2}}$, where cov_{12} is the covariance of trait means of replicate individuals of an ecotype and V_{G1} and V_{G2} are the among-ecotype variance components for those traits (see Table 2). A 95% confidence interval (in parentheses below each value of r_G) was estimated using a *z*-transformation (Sokal and Rohlf 1995, p. 577). Correlations in italics have confidence intervals *not* encompassing zero. r_G values greater than the theoretical maximum of 1.0 are statistical artifacts resulting from sampling variance, and confidence intervals for these estimates are undefined.

TABLE 4

Summary statistics for 13 inflorescence development and morphology traits for two populations of RI lines used for QTL analyses

Trait	$\overline{X} \pm$ (SD)	$[V_G]^a$	$[V_E]^b$	$[H^2]^c$	$[CV_G]^d$
		L*er* × Col RI population			
Bolting time (days)	25.30 (1.72)	2.703****	2.842	0.487	6.50
Length of reproductive phase of main axis (days)	16.73 (0.95)	0.653****	2.993	0.179	4.83
Time to maturity of main axis (days)	42.03 (1.54)	2.070****	4.381	0.321	3.42
Rosette leaves at bolting	11.04 (1.33)	1.629****	2.489	0.396	11.56
Rosette diameter (cm)	1.65 (0.19)	0.014****	0.276	0.049	7.26
Plant height (cm)	10.94 (3.69)	12.882****	11.795	0.522	32.80
Main inflorescence fruits	18.45 (2.15)	1.648***	39.952	0.040	6.96
Axillary fruits	3.22 (2.67)	2.431**	68.859	0.034	48.37
Nonelongated 2° meristems	0.76 (0.58)	0.257****	0.886	0.225	66.59
Elongated axils	0.99 (0.45)	0.125****	0.957	0.116	35.63
2° inflorescence meristems on main axis	1.75 (0.46)	0.147****	1.057	0.122	21.81
Early flowers	8.71 (2.02)	3.392****	9.929	0.255	21.16
Total fruits	24.08 (4.36)	7.232****	154.827	0.045	11.17
		Cvi × L*er* RI population			
Bolting time (days)	22.54 (4.31)	17.434****	6.003	0.744	18.52
Length of reproductive phase of main axis (days)	18.43 (2.61)	6.254****	8.047	0.437	13.57
Time to maturity of main axis (days)	41.08 (5.20)	25.311****	11.007	0.697	12.25
Rosette leaves at bolting	8.26 (1.55)	2.194****	1.913	0.534	17.93
Rosette diameter (cm)	1.71 (0.25)	0.041****	0.275	0.129	11.83
Plant height (cm)	10.18 (3.70)	12.995****	10.440	0.555	35.40
Main inflorescence fruits	13.62 (3.33)	9.438****	24.208	0.281	22.55
Axillary fruits	2.53 (3.04)	6.508****	40.212	0.139	100.69
Nonelongated 2° meristems	2.06 (0.66)	0.372****	0.889	0.295	29.57
Elongated axils	0.38 (0.35)	0.090****	0.557	0.139	79.28
2° inflorescence meristems on main axis	2.44 (0.55)	0.252****	0.689	0.268	20.58
Early flowers	4.91 (1.32)	1.560****	3.116	0.334	25.42
Total fruits	16.15 (6.00)	29.592****	94.906	0.238	33.68

[a] Among-line variance component from ANOVA; tests whether genetic differences exist among RI lines for specified traits: $^{**}P \leq 0.01$; $^{***}P \leq 0.001$; $^{****}P \leq 0.0001$.

[b] Residual variance component from ANOVA.

[c] Measure of total phenotypic variance attributable to genetic differences among lines (broad sense heritability) calculated as $V_G/(V_G + V_E)$.

[d] Coefficient of genetic variation calculated as $(100 \times \sqrt{V_G})/\overline{X}$.

lines. Similarities in trait correlations, however, were greater between the sets of RI lines than between either set and the ecotypes. The (L*er* × Col) *vs.* ecotypes and (Cvi × L*er*) *vs.* ecotypes comparisons revealed ~45 and 56%, respectively, of trait correlations with overlapping 95% confidence intervals. Despite variability among these comparisons, certain trait correlations were invariantly strong. For example, a block of correlated traits identified in the ecotypes—bolting time, rosette leaves at bolting, and time to maturity of main axis—was also observed in both sets of RI lines.

Linkage maps of *A. thaliana*: Because the two sets of RI lines used for QTL mapping have been genotyped for largely different sets of molecular markers, it was necessary to construct separate linkage maps for QTL analyses. The L*er* × Col linkage map consists of 217 markers, spans 565.65 cM, and has average intermarker distances of 2.60 cM (Figure 2). The Cvi × L*er* map consists of 138 markers, spans 458.45 cM, and has average intermarker distances of 3.32 cM (Figure 2). For both maps, marker orders were largely identical to those of previous maps based on these lines [see http://nasc.nott.ac.uk/new_ri_map.html for the current L*er* × Col RI line map and Alonso-Blanco *et al.* (1998a) for the Cvi × L*er* RI line map]. The exceptions are three order changes on the L*er* × Col map (all on chromosome 1) and a single order change on the Cvi × L*er* map (on chromosome 3). Three of these changes were order reversals of tightly linked adjacent markers and the remaining change involved a previously telomeric marker (*SNP308*) on chromosome 1 (L*er* × Col) mapping to 10.22 cM. Our revised genetic map position of *SNP308* is consistent with the physical map position of this marker (http://www.arabidopsis.org/servlets/mapper).

Chromosomal map lengths were consistently shorter in the Cvi × L*er* RI lines than in the L*er* × Col RI

TABLE 5

Genetic correlations among inflorescence development and morphology traits in RI populations derived from L*er* × Col (above diagonal) and Cvi × L*er* (below diagonal) crosses

	Total fruits	Early flowers	2° inflorescence meristems on main axis	Elongated axils	Nonelongated 2° meristems	Axillary fruits	Main inflorescence fruits	Plant height	Rosette diameter	Rosette leaves at bolting	Time to maturity of main axis	Length of reproductive phase of main axis	Bolting time
Bolting time	*−0.54* (*−0.67*, *−0.38*)	*0.25* (*0.05*, *0.43*)	*0.57* (*0.42*, *0.69*)	*−0.69* (*−0.78*, *−0.57*)	*0.91* (*0.87*, *0.94*)	*−0.34* (*−0.51*, *−0.16*)	−0.02 (−0.22, 0.18)	*−0.49* (*−0.62*, *−0.32*)	*−0.25* (*−0.43*, *−0.06*)	*0.81* (*0.73*, *0.87*)	*0.93* (*0.90*, *0.95*)	*−0.52* (*−0.65*, *−0.35*)	—
Length of reproductive phase of main axis	*0.46* (*0.29*, *0.61*)	*−0.47* (*−0.61*, *−0.30*)	*−0.51* (*−0.64*, *−0.34*)	*0.22* (*0.02*, *0.40*)	*−0.53* (*−0.66*, *−0.38*)	*0.27* (*0.07*, *0.44*)	*0.47* (*0.30*, *0.62*)	*0.51* (*0.35*, *0.65*)	*0.51* (*0.34*, *0.64*)	*−0.50* (*−0.64*, *−0.34*)	0.15 (−0.05, 0.34)	—	*0.22* (*0.07*, *0.37*)
Time to maturity of main axis	*−0.36* (*−0.52*, *−0.17*)	0.02 (−0.18, 0.22)	*0.37* (*0.18*, *0.53*)	*−0.67* (*−0.76*, *−0.54*)	*0.74* (*0.64*, *0.82*)	*−0.24* (*−0.42*, *−0.05*)	*0.24* (*0.04*, *0.42*)	*−0.27* (*−0.44*, *−0.07*)	−0.01 (−0.21, 0.19)	*0.65* (*0.52*, *0.75*)	—	*0.72* (*0.64*, *0.79*)	*0.87* (*0.83*, *0.91*)
Rosette leaves at bolting	*−0.35* (*−0.51*, *−0.16*)	*0.22* (*0.02*, *0.40*)	*0.62* (*0.48*, *0.73*)	*−0.40* (*−0.55*, *−0.21*)	*0.74* (*0.64*, *0.82*)	*−0.34* (*−0.51*, *−0.15*)	0.04 (−0.16, 0.24)	*−0.23* (*−0.41*, *−0.03*)	0.15 (−0.05, 0.34)	—	*0.86* (*0.81*, *0.89*)	*0.25* (*0.10*, *0.39*)	*0.89* (*0.86*, *0.92*)
Rosette diameter	*0.47* (*0.30*, *0.61*)	*−0.49* (*−0.62*, *−0.32*)	0.11 (−0.09, 0.30)	*0.64* (*0.50*, *0.74*)	*−0.38* (*−0.54*, *−0.19*)	*0.22* (*0.02*, *0.40*)	*0.31* (*0.11*, *0.48*)	*1.02*	—	*−0.21* (*−0.35*, *−0.06*)	*−0.31* (*−0.44*, *−0.16*)	−0.10 (−0.25, 0.05)	*−0.37* (*−0.49*, *−0.23*)
Plant height	−0.19 (−0.38, 0.01)	*−0.80* (*−0.86*, *−0.71*)	−0.15 (−0.34, 0.05)	*0.57* (*0.41*, *0.69*)	*−0.51* (*−0.64*, *−0.35*)	*−0.44* (*−0.59*, *−0.27*)	*−0.47* (*−0.61*, *−0.29*)	—	*0.60* (*0.49*, *0.69*)	−0.15 (−0.30, 0)	−0.05 (−0.20, 0.11)	*0.18* (*0.03*, *0.32*)	*−0.19* (*−0.33*, *−0.03*)
Main inflorescence fruits	*2.00*	*1.14*	−0.14 (−0.33, 0.06)	0.01 (−0.19, 0.21)	−0.12 (−0.31, 0.09)	*1.55*	—	−0.08 (−0.23, 0.08)	0.06 (−0.10, 0.21)	−0.04 (−0.19, 0.12)	*0.18* (*0.02*, *0.32*)	*0.73* (*0.65*, *0.80*)	*−0.22* (*−0.36*, *−0.07*)
Axillary fruits	*2.20*	*1.00*	−0.09 (−0.28, 0.11)	*0.49* (*0.33*, *0.63*)	*−0.41* (*−0.57*, *−0.23*)	—	*0.99* (*0.99*, *1.00*)	−0.09 (−0.25, 0.06)	0.09 (−0.07, 0.24)	*−0.33* (*−0.46*, *−0.19*)	−0.04 (−0.19, 0.12)	*0.60* (*0.50*, *0.69*)	*−0.42* (*−0.54*, *−0.29*)
Nonelongated 2° meristems	*−0.61* (*−0.72*, *−0.47*)	0.19 (−0.01, 0.37)	*0.88* (*0.83*, *0.92*)	*−0.80* (*−0.86*, *−0.72*)	—	*−0.65* (*−0.73*, *−0.55*)	*−0.23* (*−0.37*, *−0.08*)	*−0.28* (*−0.42*, *−0.13*)	*−0.18* (*−0.32*, *−0.03*)	*0.78* (*0.71*, *0.83*)	*0.56* (*0.44*, *0.65*)	−0.04 (−0.19, 0.12)	*0.73* (*0.65*, *0.79*)
Elongated axils	*0.93* (*0.90*, *0.95*)	−0.18 (−0.37, 0.02)	*0.33* (*0.14*, *0.50*)	—	*−0.71* (*−0.78*, *−0.63*)	*1.32*	*0.88* (*0.84*, *0.91*)	−0.10 (−0.25, 0.06)	0.15 (−0.01, 0.30)	*−0.38* (*−0.51*, *−0.24*)	*−0.19* (*−0.33*, *−0.03*)	*0.40* (*0.27*, *0.53*)	*−0.48* (*−0.59*, *−0.35*)
2° inflorescence meristems on main axis	0.05 (−0.15, 0.25)	0.08 (−0.12, 0.27)	—	−0.01 (−0.17, 0.14)	*0.99* (*0.99*, *0.99*)	0 (−0.15, 0.15)	*0.24* (*0.09*, *0.38*)	*−0.41* (*−0.53*, *−0.27*)	−0.13 (−0.28, 0.03)	*0.70* (*0.61*, *0.77*)	*0.54* (*0.43*, *0.64*)	*0.19* (*0.03*, *0.33*)	*0.57* (*0.46*, *0.67*)
Early flowers	*0.90* (*0.85*, *0.93*)	—	0.11 (−0.05, 0.26)	*0.63* (*0.53*, *0.72*)	*−0.23* (*−0.37*, *−0.07*)	*0.59* (*0.48*, *0.68*)	*0.56* (*0.45*, *0.66*)	*−0.60* (*−0.69*, *−0.49*)	−0.04 (−0.19, 0.12)	*−0.23* (*−0.37*, *−0.07*)	*−0.39* (*−0.51*, *−0.25*)	*−0.19* (*−0.33*, *−0.03*)	*−0.34* (*−0.47*, *−0.20*)
Total fruits	—	*0.60* (*0.49*, *0.69*)	0.14 (−0.02, 0.28)	*1.11*	*−0.44* (*−0.55*, *−0.30*)	*1.22*	*1.13*	−0.09 (−0.24, 0.07)	0.07 (−0.08, 0.22)	*−0.18* (*−0.33*, *−0.03*)	0.08 (−0.08, 0.23)	*0.69* (*0.61*, *0.77*)	*−0.33* (*−0.46*, *−0.18*)

Genetic correlations (r_G) were calculated as $cov_{12}/\sqrt{V_{G1}V_{G2}}$, where cov_{12} is the covariance of trait means of replicate individuals of a RI line, and V_{G1} and V_{G2} are the among-line variance components for those traits (see Table 4). A 95% confidence interval (in parentheses below each value of r_G) was estimated using a *z*-transformation (Sokal and Rohlf 1995, p. 577). Correlations in italics have confidence intervals *not* encompassing zero. r_G values greater than the theoretical maximum of 1.0 are statistical artifacts resulting from sampling variance, and confidence intervals for these estimates are undefined.

lines. This difference may be attributable to (i) reduced recombination in the Cvi × L*er* RI lines, (ii) reduced marker coverage in telomeric regions for the Cvi × L*er* RI lines, (iii) a larger number of genotype scoring errors in the L*er* × Col data set (inflation of map length), or (iv) some combination of these factors. Some of the integrating markers (those mapped in both sets of RI lines) did not map to unique positions given the criteria set during map construction. These markers were not used for QTL mapping but are included on the linkage maps (in the genetic interval of highest likelihood) for map comparisons (Figure 2) and are indicated as open symbols.

Numbers and magnitude of inflorescence development QTL: The two mapping populations provided an opportunity to map loci that contribute to quantitative genetic variation in inflorescence developmental patterns in Arabidopsis. Detection of QTL is necessarily restricted to genetic variation segregating between lines used to construct mapping populations. A larger sample of genetic variation can be explored by examining more than one mapping population. QTL for 13 inflorescence development and morphology traits detected by CIM in two sets of RI lines are depicted graphically in Figure 2 and are listed in Tables 6 and 7.

A total of 47 QTL were detected in the L*er* × Col RI lines and 63 QTL were detected in the Cvi × L*er* RI lines. The larger number of QTL detected in the Cvi × L*er* RI lines may be attributable to increased statistical power associated with the larger number of lines (160 Cvi × L*er* lines *vs.* 97 L*er* × Col lines) and/or different QTL alleles segregating in the two mapping populations. For each trait, between 1 and 6 and between 1 and 8 QTL were detected in the L*er* × Col and Cvi × L*er* RI lines, respectively. Where multiple QTL were detected for a trait, allele effects were usually both positive and negative (Tables 6 and 7). Thus, the direction of allele effects was not consistently in the direction of the relative differences among parental lines. This phenomenon is commonly observed in QTL studies (reviewed in Tanksley 1993; Lynch and Walsh 1998) and the sorting of these alleles likely explains transgressive segregation in progeny of genetically differentiated parental lines (Rieseberg *et al.* 1999).

The amount of phenotypic variance explained by QTL varied greatly in both sets of RI lines. Individual QTL account for 2.1–68.4% of phenotypic variance in the L*er* × Col RI lines and 1.2–67.4% of phenotypic variance in the Cvi × L*er* RI lines (Tables 6 and 7). The individual QTL explaining the most variance in each set of RI lines mapped to the same region on chromosome 2 (near *er*) and explained variance in the same trait (plant height). These QTL (and others mapping to this same region) are likely attributable to the *erecta* mutation, which segregates in both sets of RI lines and affects inflorescence architecture. *erecta* is not a naturally occurring mutation, however, but rather was generated in the laboratory through mutagenesis. If QTL mapping to *erecta* are removed from the analysis, the remaining QTL (representing natural variation) account for 2.1–35.6% of phenotypic variance in the L*er* × Col RI lines and 1.2–19.5% of phenotypic variance in the Cvi × L*er* RI lines.

A distribution of standardized QTL effects is illustrated in Figure 3 (data combined across all traits and sets of RI lines). QTL mapping to the *erecta* mutation are included but are indicated by shaded regions of the histogram bars. Overall, the largest proportion of QTL detected were of relatively small effect and large-effect QTL were relatively rare. This result is consistent with findings of other QTL studies documenting that most differences between lines are due to a small number of QTL of large effect accompanied by a larger number of QTL of smaller effect (reviewed in Tanksley 1993; Falconer and Mackay 1996; Lynch and Walsh 1998). The apparent decline of QTL in the class of smallest effect should not be interpreted as evidence that small effect QTL are rare, but rather simply reflects the statistical difficulties of detecting these loci.

Clustering of QTL was evident and consistent with strong genetic correlations among inflorescence development traits: QTL for inflorescence development traits mapped to all five Arabidopsis chromosomes in both sets of RI lines. Despite this genome-wide distribution, a large proportion of QTL had overlapping 2-LOD support limits (Figure 2) and were clustered in specific chromosomal regions (*i.e.*, at the top and bottom of chromosomes 1 and 5 and middle of chromosome 2). Clustering of QTL was not unexpected given the strong genetic correlations observed among many inflorescence development traits (Table 5). This pattern was especially evident for QTL of larger magnitude. It is not possible with the resolution of QTL mapping to determine whether these patterns result from pleiotropic effects of single genes or tight linkage. Only when these QTL have been resolved to the level of the gene and, eventually, molecular variants within genes, will it be possible to discover with any degree of confidence the underlying genetic mechanisms involved in these correlations.

Comparisons of the L*er* × Col and Cvi × L*er* maps reveal that QTL for many of the same traits appear to map to similar regions of chromosomes (*e.g.*, QTL for rosette diameter, plant height, main inflorescence fruits, axillary fruits, elongated axils, and early flowers on chromosome 2 and QTL for bolting time, time to maturity of main axis, and nonelongated secondary meristems on chromosome 5). Alleles of the Landsberg *erecta* ecotype segregate in both sets of RI lines and thus it is plausible that these patterns are due to segregation of the same genetic factor(s). Indeed, on chromosome 2, the actual *erecta* mutation (marker *er*) maps nearest those QTL in both L*er* × Col and Cvi × L*er* and is likely the genetic factor responsible. However, because these

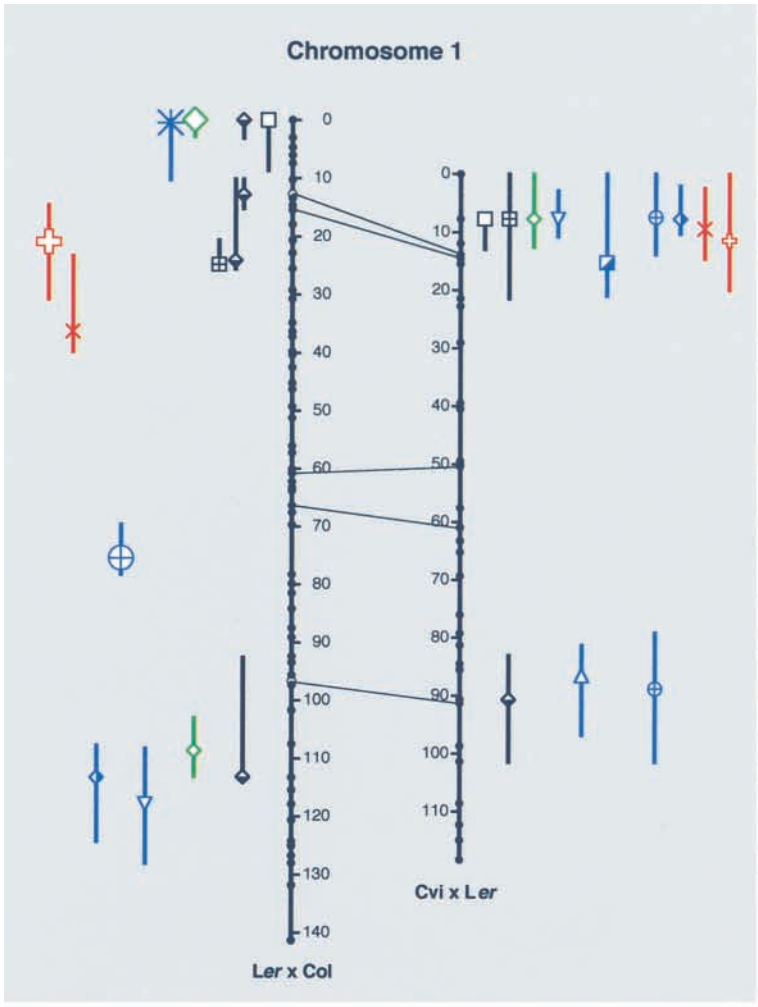
Chromosome 1
Ler x Col
Cvi x Ler

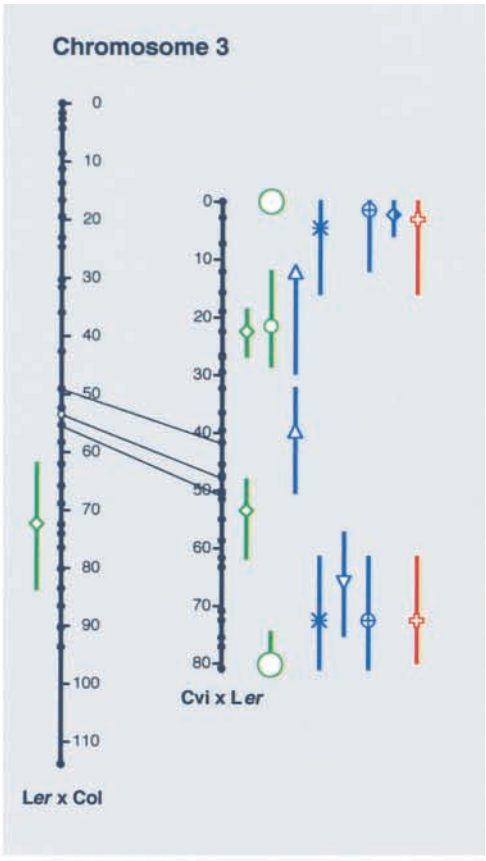
Chromosome 3
Cvi x Ler
Ler x Col

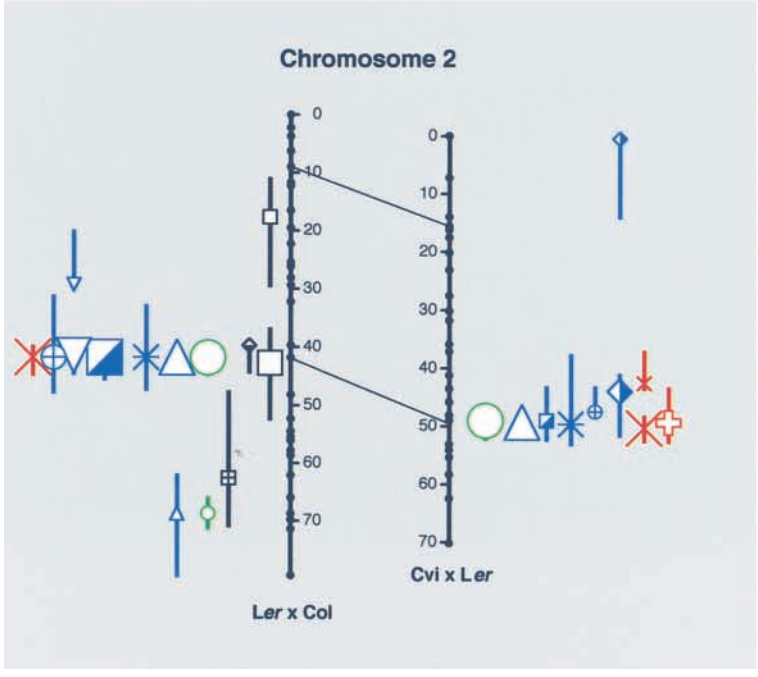
Chromosome 2
Ler x Col
Cvi x Ler

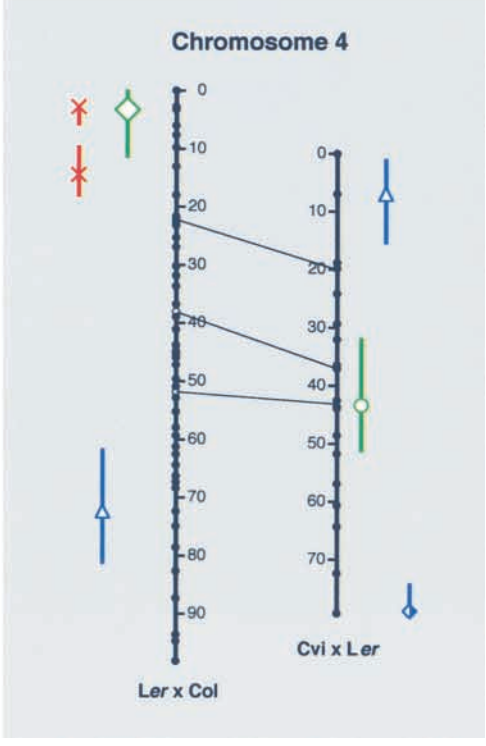
Chromosome 4
Ler x Col
Cvi x Ler

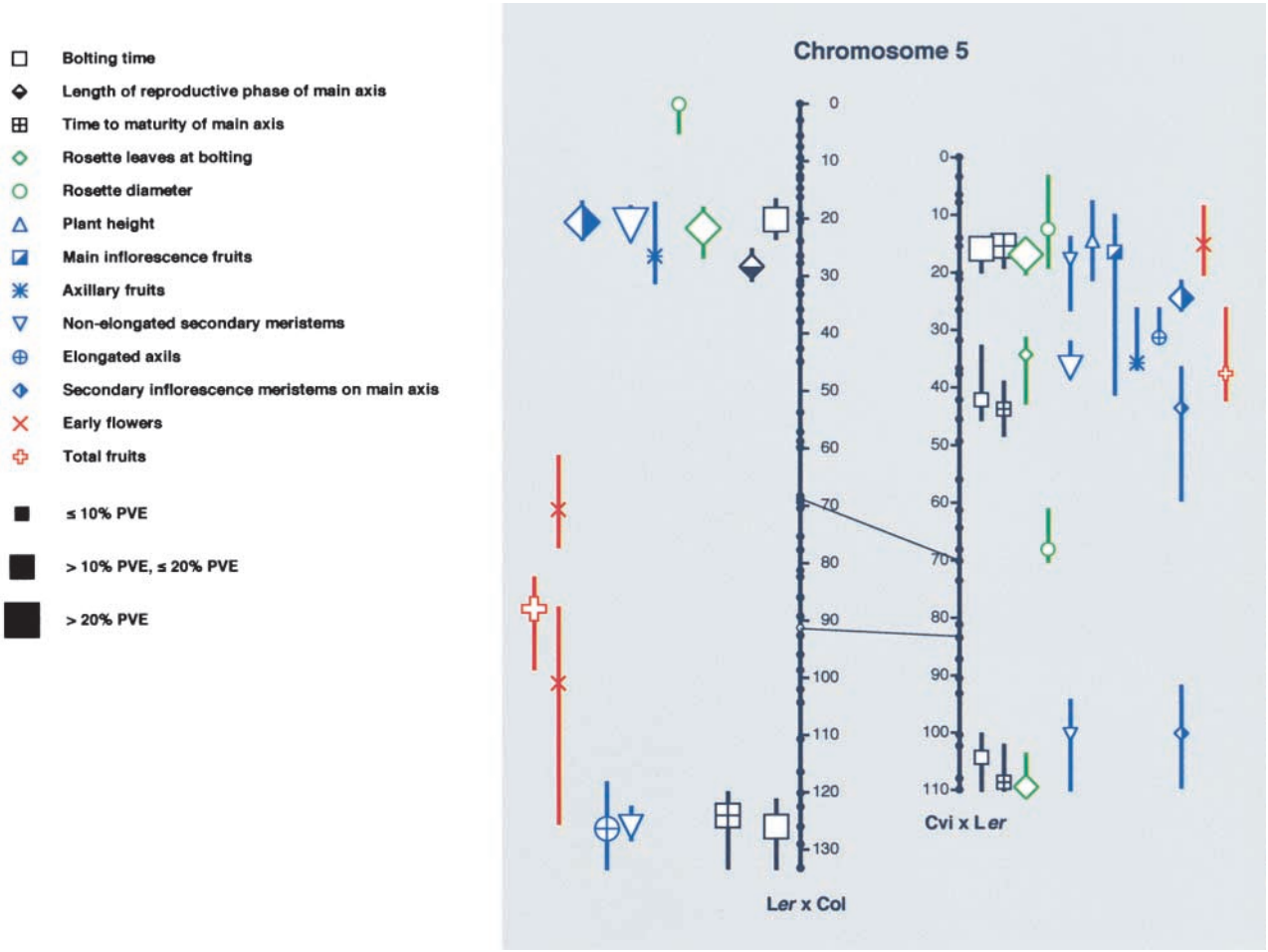

FIGURE 2.—*Continued.*

maps are based on largely different sets of molecular markers, QTL positions (and 2-LOD support limits) cannot be directly compared across the L*er* × Col and Cvi × L*er* maps unless, as with *er*, markers used to define QTL (or 2-LOD support limits) are used in both mapping populations.

QTL on chromosomes 1 and 5 have epistatic effects in the Cvi × L*er* RI lines: Tests for epistasis among QTL revealed no significant interactions in the L*er* × Col RI lines but five significant two-way interactions and one significant three-way interaction in the Cvi × L*er* RI lines (Figures 4 and 5). Where significant interactions affected more than one trait, the nature of the interaction across traits was strikingly similar (Figure 5, A–C). This latter result is perhaps not surprising, given that the traits affected by these interactions—bolting time, time to maturity of main axis, rosette leaves at bolting, and nonelongated secondary meristems—were highly correlated in the Cvi × L*er* RI lines (average $r_G = 0.78$).

The interaction effect of markers *BH.325* and *DF.184* on two traits (rosette leaves at bolting and nonelongated secondary meristems) was especially noteworthy. When the genotype of marker *BH.325* is L*er*, phenotypic values are virtually identical irrespective of the genotype of marker *DF.184*. However, when the genotype of marker *BH.325* is Cvi, the phenotype is strongly dependent on

FIGURE 2.—*A. thaliana* genetic linkage maps constructed from the L*er* × Col (left chromosomes) and Cvi × L*er* (right chromosomes) RI lines and QTL positions for 13 inflorescence development and morphology traits. QTL for different traits are depicted with different symbols and vertical lines associated with each QTL indicate 2-LOD support limits. Symbol size is proportional to the amount of variance explained by the QTL. Colors of QTL are associated with trait subcategories as follows: black, inflorescence developmental timing; green, basal rosette morphology; blue, inflorescence architecture; red, fitness. These categories are not mutually exclusive as many traits could be classified in more than one category. Genetic markers are depicted as round symbols on chromosomes. Markers connected by lines were mapped in both sets of RI lines and represent landmarks for map comparisons. Markers represented as open symbols did not map to unique intervals, given the mapping criteria, and are placed here in the interval of highest likelihood. These markers were not used in QTL analyses. Units of map length are in centimorgans.

TABLE 6

QTL for 13 inflorescence development and morphology traits mapped in L*er* × Col RI lines

Trait	Chromosome	QTL map position, cM (nearest marker)	2-LOD support limit, cM range (flanking markers)[a]	Additive effect[b]	$[r^2]$[c]
Bolting time	1	0.01 (*ve001*)	0–8.60 (*ve001–SNP308*)	−0.53	0.083
	2	17.65 (*g4133*)	11.12–29.39 (*DF.225L–mi148*)	0.58	0.085
	2	42.71 (*er*)	37.02–52.32 (*mi238–ve096*)	−0.61	0.109
	5	20.15 (*ve033*)	16.80–23.36 (*KG31–mi174*)	0.99	0.162
	5	126.01 (*SNP153*)	121.44–133.20 (*ve032–BIO205*)	0.74	0.187
Length of reproductive phase of main axis	1	0.01 (*ve001*)	0–3.06 (*ve001–T1G11a*)	0.38	0.067
	1	12.83 (*mi443*)	10.20–15.16 (*SNP308–BH.147L*)	−0.43	0.085
	1	24.12 (*EG17G9*)	10.20–25.54 (*SNP308–mi113*)	−0.34	0.079
	1	113.19 (*mi185*)	92.60–113.66 (*mi259–mi103*)	0.22	0.045
	2	39.69 (*GPA1*)	39.62–44.21 (*GPA1–mi54*)	0.40	0.088
	5	28.34 (*mi322*)	25.47–30.64 (*mi174–g4560*)	−0.49	0.203
Time to maturity of main axis	1	24.82 (*EG17G9*)	20.66–25.54 (*ve007–mi113*)	−0.64	0.073
	2	62.57 (*g4514*)	47.81–70.77 (*mi54–mi79a*)	−0.48	0.079
	5	124.03 (*g2368*)	120.14–133.06 (*ve032–BIO205*)	0.72	0.195
Rosette leaves at bolting	1	0.01 (*ve001*)	0–2.81 (*ve001–T1G11a*)	−0.60	0.178
	1	108.69 (*mi185*)	103.01–113.09 (*m315–Tag1*)	0.49	0.103
	3	72.37 (*AtPK41A*)	61.98–83.51 (*g4117–g2778*)	0.34	0.058
	4	3.28 (*mi122*)	0.11–11.26 (*mi51–app*)	−0.49	0.120
	5	21.66 (*CDs5*)	18.20–26.61 (*KG31–cor6.6*)	0.87	0.356
Rosette diameter	2	41.81 (*er*)	41.79–44.71 (*er–mi54*)	0.12	0.309
	2	68.71 (*Ubique*)	66.09–71.17 (*m336–mi79a*)	−0.07	0.076
	5	0.01 (*pAtT80*)	0–4.89 (*pAtT80–g3715*)	0.06	0.085
Plant height	2	41.79 (*er*)	39.99–44.51 (*GPA1–mi54*)	3.69	0.684
	2	68.69 (*Ubique*)	62.17–79.29 (*g4514–RRS2*)	−0.60	0.021
	4	72.34 (*CDs11*)	61.85–81.07 (*mi422–m214*)	−0.66	0.027
Main inflorescence fruits	2	41.79 (*er*)	39.79–45.41 (*GPA1–mi54*)	−1.12	0.250
Axillary fruits	1	0.51 (*ve001*)	0–10.20 (*ve001–SNP308*)	0.95	0.114
	2	41.79 (*er*)	33.02–47.21 (*mi238–mi54*)	−1.03	0.125
	5	26.51 (*cor6.6*)	17.30–31.02 (*KG31–TSL*)	−1.29	0.088
Nonelongated 2° meristems	1	117.88 (*CD.173L*)	108.29–128.01 (*mi185–agp64*)	0.14	0.055
	2	29.32 (*mi139*)	20.23–29.39 (*PR1–mi148*)	0.21	0.079
	2	41.49 (*er*)	39.69–44.51 (*mi238–mi54*)	−0.33	0.209
	5	21.16 (*CDs5*)	17.90–23.66 (*KG31–mi174*)	0.28	0.215
	5	126.01 (*SNP153*)	122.63–128.11 (*g2368–CATHANK*)	0.31	0.147
Elongated axils	1	75.41 (*mi72*)	69.66–78.22 (*mi133–mi291a*)	0.16	0.120
	2	41.79 (*er*)	31.39–47.71 (*mi148–mi54*)	0.16	0.109
	5	126.31 (*SNP153*)	118.35–133.20 (*ATR3–BIO205*)	−0.16	0.119
2° inflorescence meristems on main axis	1	113.26 (*Tag1*)	107.79–124.28 (*mi185–mi425*)	0.13	0.070
	5	20.55 (*CDs5*)	17.10–23.46 (*KG31–mi174*)	0.25	0.235
Early flowers	1	36.37 (*DF.73L*)	23.32–39.80 (*BH.147L–mi265*)	0.45	0.045
	2	41.79 (*er*)	39.99–44.71 (*GPA1–mi54*)	−1.67	0.420
	4	2.76 (*mi204*)	2.71–5.68 (*mi204–g3843*)	−0.48	0.043
	4	14.47 (*app*)	9.76–17.97 (*mi390–Gsl_ohp*)	−0.78	0.078
	5	70.63 (*m247*)	61.40–76.97 (*mi137–mCH1*)	0.43	0.043
	5	100.9 (*h2a1*)	87.79–125.23 (*ve027–SNP153*)	−0.43	0.039
Total fruits	1	20.96 (*ve007*)	14.66–30.75 (*ATTSO477–g3829*)	1.59	0.136
	5	87.89 (*ve027*)	82.60–98.25 (*mi83–m435*)	−2.01	0.144

[a] Markers nearest (but outside of) the 2-LOD support limits.

[b] The additive effect (a) of a QTL is defined as $(Q_1Q_1 - Q_2Q_2)/2$, where Q_1Q_1 and Q_2Q_2 represent the mean phenotypes of RI lines homozygous for alternative genotypes at a QTL position. The sign of the additive effect corresponds to the direction of effect of the Columbia allele on the phenotype.

[c] Proportion of variance explained by the QTL after accounting for background markers.

the genotype of marker *DF.184*. This conditional neutrality may be of evolutionary importance, since it suggests that in some circumstances, allelic effects may be dependent on genetic context. The rate at which naturally occurring alleles under selection are fixed in (or lost from) a population may be slowed due to this phenomenon.

The single significant three-way interaction involved

TABLE 7

QTL for 13 inflorescence development and morphology traits mapped in Cvi × L*er* RI lines

Trait	Chromosome	Map position, cM (nearest marker)	2-LOD support limit, cM range (flanking markers)[a]	Additive effect[b]	$[r^2]$[c]
Bolting time	1	7.71 (*AXR-1*)	7.61–12.84 (*PVV4–DF.162L*)	1.35	0.091
	5	15.9 (*BH.325L*)	14.32–19.8 (*FD.239L–BH.107L*)	−2.22	0.195
	5	42.15 (*GH.121L*)	32.91–45.45 (*DF.184L–DF.154C*)	−1.33	0.076
	5	104.32 (*BF.168L*)	100.35–109.9 (*HH.143C–GD.222C*)	1.07	0.049
Length of reproductive phase of main axis	1	90.67 (*HH.375L*)	83.1–101.38 (*EC.88C–GH.157L*)	−0.64	0.054
Time to maturity of main axis	1	7.71 (*AXR-1*)	0.01–21.41 (*PVV4–CC.120C*)	1.06	0.038
	5	15.4 (*BH.325L*)	14.32–19 (*FD.239L–BH.107L*)	−2.53	0.175
	5	43.75 (*GH.121L*)	39.16–48.19 (*GH.117C–HH.480C*)	−1.56	0.073
	5	108.65 (*DF.119L*)	102.27–109.9 (*BF.168L–GD.222C*)	1.41	0.056
Rosette leaves at bolting	1	7.71 (*AXR-1*)	0.01–12.44 (*PVV4–DF.162L*)	0.30	0.035
	3	22.46 (*GH.390L*)	18.72–26.56 (*CC.110L–HH.158L*)	0.33	0.037
	3	53.45 (*HH.117C*)	48.21–61.64 (*AD.108L–GH.172C*)	−0.38	0.041
	5	16.90 (*BH.325L*)	14.52–20.20 (*FD.239L–BH.107L*)	−0.83	0.212
	5	34.31 (*DF.184L*)	31.54–42.65 (*DF.184L–DF.154C*)	−0.54	0.086
	5	109.45 (*GD.222C*)	103.82–109.45 (*BF.168–GD.222C*)	0.53	0.113
Rosette diameter	2	49.03 (*er*)	46.88–52.13 (*FD.150C–AD.191L*)	−0.12	0.210
	3	0.01 (*DF.77C*)	0–1.71 (*DF.77C–GB.120C*)	−0.11	0.155
	3	21.49 (*GH.390L*)	12.09–28.3 (*FD.111L–GD.318C*)	0.09	0.082
	3	80.18 (*AD.112L*)	74.67–80.78 (*DF.65L–AD.112L*)	0.09	0.123
	4	43.44 (*g4539*)	32.07–51.12 (*FD.154L–FD.167L*)	−0.06	0.058
	5	12.51 (*FD.239L*)	3.4–19.1 (*CH.690C–BH.107L*)	0.06	0.059
	5	68.11 (*CH.88L*)	61.29–70.1 (*EC.395C–CD.116L*)	−0.07	0.075
Plant height	1	86.51 (*GD.160C*)	81.3–96.72 (*EC.88C–BF.116C*)	−0.54	0.020
	2	49.33 (*er*)	48.27–50.83 (*GD.460L–AD.191L*)	−3.16	0.674
	3	12.09 (*FD.111L*)	12.06–29.47 (*FD.111L–GD.318C*)	0.56	0.013
	3	39.6 (*GB.210L*)	32.32–50.12 (*AD.92L–HH.440L*)	−0.44	0.012
	4	6.98 (*GH.250C*)	1.21–15.28 (*ANL2–CH.169C*)	0.56	0.021
	5	14.52 (*FD.239L*)	7.81–21.17 (*BH.144L–BF.269C*)	0.53	0.017
Main inflorescence fruits	1	15.24 (*EC.480C*)	0–20.9 (*DF.162L–CC.120C*)	−1.02	0.090
	2	49.03 (*er*)	43.4–52.23 (*GB.150L–AD.191L*)	1.06	0.098
	5	16.5 (*BH.325L*)	10.21–41.06 (*BH.144L–GH.121L*)	0.91	0.058
Axillary fruits	2	49.63 (*er*)	37.84–53.03 (*BF.221L–AD.191L*)	1.02	0.108
	3	4.50 (*GB.120C*)	0–15.72 (*DF.77C–CC.266L*)	−0.85	0.072
	3	72.46 (*DF.65L*)	61.56–80.8 (*GH.172C–HH.90L*)	−0.78	0.062
	5	35.81 (*DF.184L*)	26.46–36.69 (*DF.231C–GH.473C*)	0.78	0.060
Nonelongated 2° meristems	1	7.71 (*AXR-1*)	2.91–10.71 (*PVV4–HH.335C*)	0.21	0.089
	3	65.95 (*FD.98C*)	57.36–74.97 (*HH.117C–AD.495L*)	0.17	0.063
	5	17.8 (*BH.325L*)	14.01–26.46 (*FD.239L–DF.231C*)	−0.21	0.064
	5	36.61 (*DF.184L*)	32.21–36.69 (*DF.231C–GH.473C*)	−0.26	0.121
	5	100.35 (*HH.143C*)	94.45–109.9 (*FD.345C–GD.222C*)	0.16	0.057
Elongated axils	1	7.41 (*AXR-1*)	0–13.74 (*PVV4–DF.162L*)	−0.10	0.071
	1	88.81 (*HH.375L*)	79.12–101.38 (*DF.260L–GH.157L*)	−0.09	0.058
	2	47.48 (*FD.150C*)	43.4–48.07 (*GB.150L–GD.460L*)	0.12	0.095
	3	1.41 (*GB.120C*)	0–11.76 (*DF.77C–FD.111L*)	−0.09	0.063
	3	72.46 (*DF.65L*)	61.56–80.8 (*GH.172C–HH.90L*)	−0.08	0.049
	5	31.44 (*DF.184L*)	26.46–31.81 (*DF.231C–DF.184L*)	0.09	0.053
2° inflorescence meristems on main axis	1	7.71 (*AXR-1*)	2.01–10.21 (*PVV4–HH.335C*)	0.13	0.056
	2	0.51 (*AD.156C*)	0.01–13.98 (*AD.156C–GH.580L*)	0.11	0.038
	2	43.99 (*GB.150L*)	41.20–51.53 (*FD.85C–AD.191L*)	0.21	0.139
	3	2.01 (*GB.120C*)	0–5.7 (*DF.77C–EG.75L*)	−0.15	0.066
	4	78.88 (*BH.342C*)	74.38–78.88 (*GB.750C–BH.342C*)	0.12	0.040
	5	24.56 (*AD.114C*)	21.67–26.54 (*BF.269C–DF.231C*)	−0.23	0.157
	5	43.65 (*GH.121L*)	36.69–59.47 (*GH.473C–EC.395C*)	−0.14	0.047
	5	100.15 (*HH.143C*)	92.00–109.45 (*CC.262C–GD.222C*)	0.13	0.049

(*continued*)

TABLE 7

(Continued)

Trait	Chromosome	Map position, cM (nearest marker)	2-LOD support limit, cM range (flanking markers)[a]	Additive effect[b]	$[r^2]$[c]
Early flowers	1	9.41 (*AXR-1*)	2.41–14.5 (*PVV4–BH.147L*)	−0.31	0.052
	2	42.6 (*FD.85C*)	37.24–43.49 (*BF.221L–GB.150L*)	0.51	0.103
	2	50.33 (*er*)	48.37–52.53 (*GD.460L–AD.191L*)	0.79	0.280
	5	15.22 (*BH.325L*)	8.71–20.3 (*BH.144L–BF.269C*)	0.37	0.064
Total fruits	1	11.41 (*HH.335C*)	0–19.9 (*PVV4–CC.120C*)	−1.56	0.064
	2	49.33 (*er*)	43.49–52.63 (*GB.150L–AD.191L*)	2.05	0.110
	3	3.00 (*GB.120C*)	0–15.72 (*DF.77C–CC.266L*)	−1.44	0.053
	3	72.46 (*DF.65L*)	61.56–79.68 (*GH.172C–HH.90L*)	−1.48	0.058
	5	37.66 (*GH.117C*)	26.46–42.15 (*DF.231C–GH.121L*)	1.54	0.060

[a] Markers nearest (but outside of) the 2-LOD support limits.
[b] The additive effect (a) of a QTL is defined as $(Q_1Q_1 - Q_2Q_2)/2$, where Q_1Q_1 and Q_2Q_2 represent the mean phenotypes of RI lines homozygous for alternative genotypes at a QTL position. The sign of the additive effect corresponds to the direction of effect of alleles from the Landsberg *erecta* ecotype.
[c] Proportion of variance explained by the QTL after accounting for background markers.

markers *AXR1*, *BH.325L*, and *GH.121L* and had effects on both bolting time (ANOVA, $F = 6.09$, $P < 0.0148$) and time to maturity of main axis (ANOVA, $F = 7.71$, $P < 0.0062$). Note that the three-way interaction is composed mostly of markers with significant two-way interactions on these same traits (Figure 4). The significant two-way combinations were included in the ANOVA models testing for significant three-way interactions.

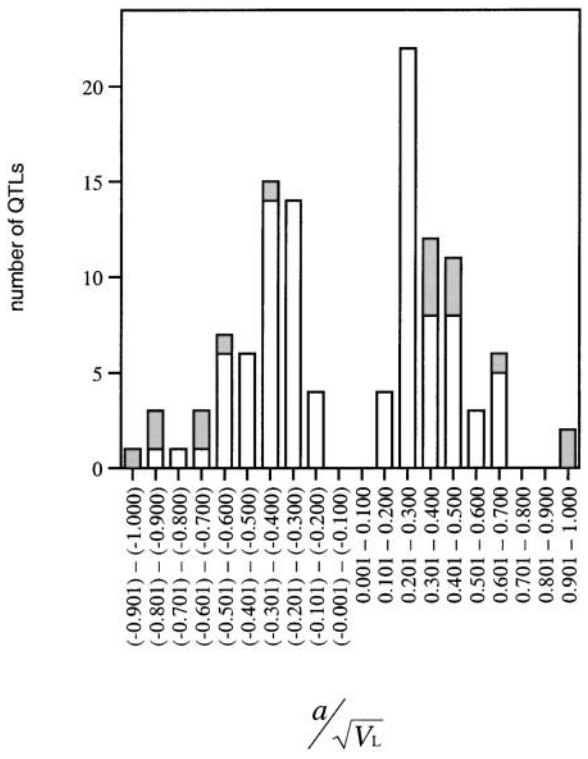

FIGURE 3.—Distribution of standardized effects of QTL for all traits across both sets of RI lines. Shaded regions of histogram bars indicate effects of QTL mapping on the *erecta* mutation.

Two of the markers (*BH.325L* and *GH.121.L*) involved in these interactions have been identified previously with interaction effects on flowering time, rosette leaf number, cauline leaf number, and total leaf number in a separate study of these lines (ALONSO-BLANCO *et al.* 1998b). In the current study, these markers were jointly involved in a significant two-way interaction (affecting bolting time and time to maturity of main axis) and comprised two of the three markers involved in the single significant three-way interaction (Figure 4). Taken separately, however, one or the other was involved in all significant interactions with the exception of a single two-way interaction (Figure 4).

The amount of phenotypic variance explained by QTL interaction effects relative to QTL main effects was evaluated by comparing type III sums of squares of interaction and main effects of markers to the total type III sums of squares in each ANOVA model. In models examining two-way marker combinations, only one interaction effect (*BH.325L* × *DF.184L*, which affected rosette leaves at bolting) explained approximately as much variance as corresponding main effects of markers (23.6% *vs.* 24.7% of variance explained by the interaction and largest main effect, respectively). In ANOVA models examining combined two-way and three-way interactions, main effects always explained considerably more variance than either two-way or three-way interactions. Thus, although multiple significant interactions were detected in the Cvi × L*er* RI lines, in the majority of instances main effects of QTL accounted for more total variance than epistatic effects.

DISCUSSION

We broadly surveyed four classes of traits associated with Arabidopsis reproductive development: inflores-

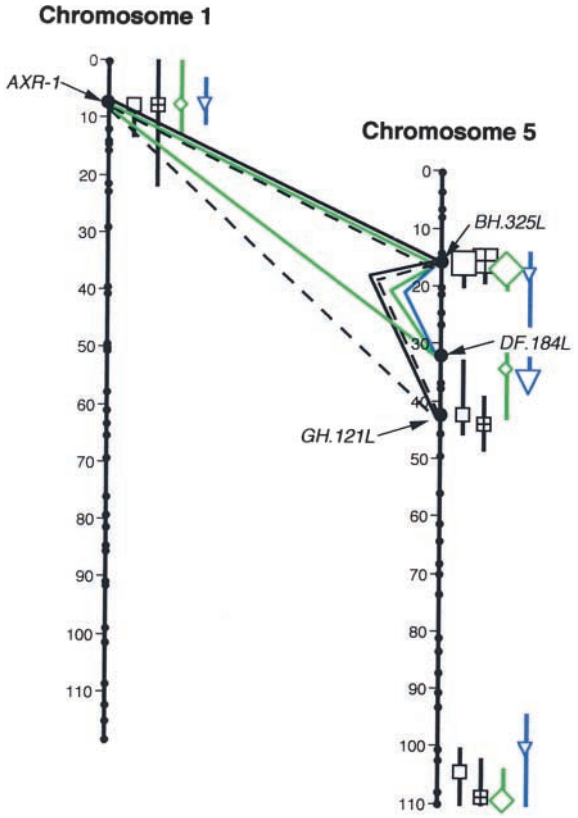

FIGURE 4.—Epistatic interactions detected in the Cvi × L*er* RI mapping population. Lines connect different pairwise combinations of markers (QTL) with significant epistatic effects on specified traits. Precise positions of QTL are shown to the right of the chromosomes (notation is the same as in Figure 2). Markers *AXR-1*, *BH.325L*, and *GH.121L* have a significant three-way interaction on both bolting time and time to maturity of main axis. Solid line, digenic interaction affecting bolting time; dashed line, digenic interaction affecting time to maturity of main axis; green line, digenic interaction affecting rosette leaves at bolting; blue line, digenic interaction affecting nonelongated secondary meristems.

cence architecture, developmental timing, rosette morphology, and reproductive fitness traits. Several aspects of inflorescence development, such as bolting time and number of rosette leaves at bolting, have already been the subject of extensive investigation (Lee *et al.* 1993; Kowalski *et al.* 1994; Clarke *et al.* 1995; Mitchell-Olds 1996; Sanda *et al.* 1997; Koornneef *et al.* 1998a,b). Other quantitative features of inflorescence development in Arabidopsis, however, have been less well characterized. Nevertheless, it is clear that naturally occurring variation in elements of inflorescence shoot architecture and developmental timing exists within this species.

Mapping populations of recombinant inbred lines have been generated between several ecotypes and have proven useful for mapping QTL in *A. thaliana* (Jansen *et al.* 1995; Mitchell-Olds 1996; Alonso-Blanco *et al.* 1998b; Mitchell-Olds and Pedersen 1998; Stratton 1998; Swarup *et al.* 1999; Juenger *et al.* 2000). Although previous studies using these lines limited their analyses to fewer (and mostly different) traits, considerable overlap of results was found between this study and one of these earlier studies. Using the Cvi × L*er* RI lines, Alonso-Blanco *et al.* (1998b) mapped QTL for flowering time, number of rosette leaves, number of cauline leaves, and total leaf number under different day-length and/or vernalization conditions. Four main QTL were detected with effects on all traits in most environments. These QTL were designated *EDI*, *FLC/FLF*, *FLG*, and *FLH* and mapped to the top of chromosome 1 and to the top, middle, and bottom of chromosome 5, respectively. This same set of QTL was detected in our study and affected (as a set) bolting time and time to maturity of main axis (Figure 2, Table 7). Individually, these QTL were also found to have effects on many additional traits in our study (*e.g.*, QTL *EDI* fell within the 2-LOD support limits of 8 of the 13 traits measured).

Clustering of QTL was evident in our study and likely reflects a similar underlying genetic basis of many inflorescence development traits. Indeed, this result is buttressed by the finding of strong genetic correlations among several inflorescence developmental phenotypes. It is interesting to note that several strong correlations span our presumed phenotypic categories (developmental timing, inflorescence architecture, etc.), perhaps indicating that, developmentally, these are artificial boundaries. It remains unclear, however, whether these correlations are due to pleiotropy or to the presence of closely linked loci in the same genomic region. If the former, then such correlations as between bolting time and elongated axils may suggest common genetic bases underlying ontogenetic timing and shoot inflorescence morphology. The existence of common genetic underpinnings for different inflorescence developmental traits is also indicated by epistasis among QTL detected in our study. Epistatic interactions among QTL were detected in the Cvi × L*er* RI lines between and within regions on chromosomes 1 and 5. Several of these interactions affected more than one trait and in these instances the nature of the interaction was strikingly similar across traits.

The overall epistatic contribution to inflorescence development traits may be underestimated in this study for two reasons. First, tests for epistasis were restricted to QTL with significant additive effects only. Although global scans for epistasis are possible (evaluating all pairwise combinations of markers), they are not always practical because of statistical problems associated with the large number of tests needed to conduct them. Global scans for epistasis can be conducted using permutations to establish significance thresholds and it will be interesting to determine whether this type of analysis can uncover other epistatic interactions for inflorescence development. Second, and more generally, the ANOVA methods used to detect epistasis may be biased *against* finding significant interactions because the stan-

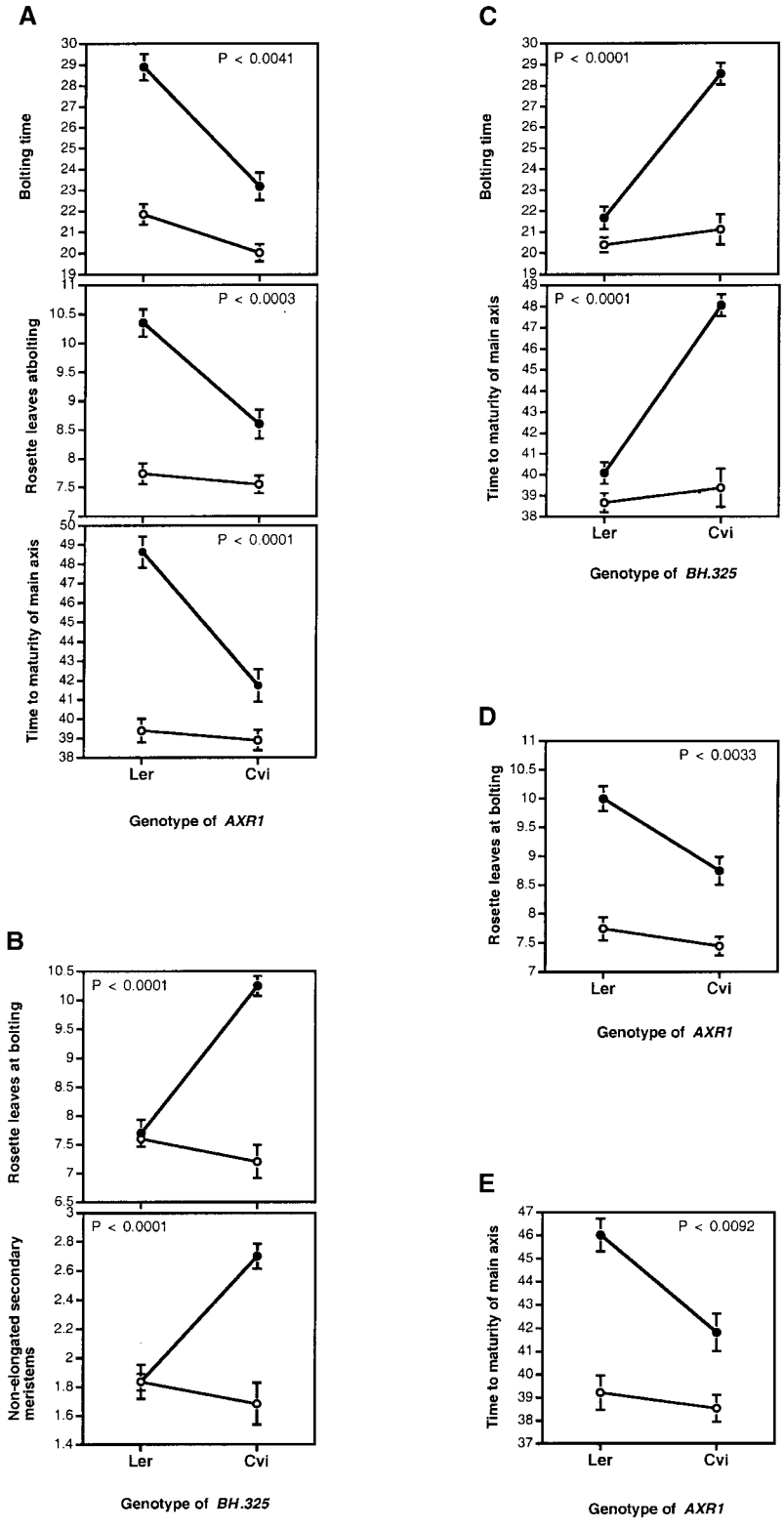

FIGURE 5.—QTL with significant epistatic interactions in the (●) Cvi × (○) L*er* RI lines. Values represent two-locus genotype means ±SE. (A) *AXR1* × *BH.325*; (B) *BH.325* × *DF.184*; (C) *BH.325* × *GH.121*; (D) *AXR1* × *DF.184*; (E) *AXR1* × *GH.121*.

dard errors associated with interaction effects can be larger than those associated with main effects (WADE 1992).

An ultimate goal of this work will be to identify, at the molecular level, genes underlying naturally occurring variation in inflorescence development traits. Isolation of the genes and genetic polymorphisms that result in naturally occurring quantitative variation in inflorescence developmental phenotypes may reveal the molecular mechanisms behind ecologically and evolutionarily

relevant architectural and phenological phenotypes. This approach also holds promise in identifying new loci in inflorescence developmental pathways and in analyzing the evolutionary origins, histories, and forces that characterize these developmental genes.

The recently completed sequence of *A. thaliana* provides a physical map of the highest resolution (Arabidopsis Genome Initiative 2000) and permits us to scan chromosomal regions identified as harboring QTL and to isolate putative positional candidate loci. On the basis of the QTL analyses, we examined three genomic regions in closer detail: (i) the top of chromosome 1 and (ii) the top and (iii) bottom of chromosome 5. These three regions contain QTL for more than one inflorescence development trait (see Figure 2). The region on the top of chromosome 1 is centered at the ~5-cM map position, is delineated by markers *ve001* and *SNP308*, and encompasses 10.2 cM. This region harbors QTL for four inflorescence development traits: bolting time, length of the reproductive phase, number of rosette leaves at bolting, and number of axillary fruits. Although representing <2% of the total Arabidopsis genetic map length, this genomic region is 3.32 Mb in length and contains 722 genes. The chromosomal region at the top of chromosome 5 is centered at map position ~21 cM and flanked by markers *mi97* and *cor6.6*. This region is 11.81 cM long (~2.1% of the genetic map length) and harbors QTL for four traits: bolting time, number of rosette leaves at bolting, nonelongated secondary meristems, and number of secondary inflorescence meristems. This region contains 3.56 Mb and 783 genes. The final region of interest is at the bottom of chromosome 5 centered on map position 127 cM. This genomic region is flanked by marker *ve023* and extends to marker *BIO205* at the tip of chromosome 5. This region contains QTL for three traits, including bolting time, time to maturity of main axis, and nonelongated secondary meristems. This region is ~13.07 cM (~2.3% of the genetic map length), encompasses a physical distance of 1.35 Mb, and contains 375 genes.

Several genes in these regions are known from previous genetic studies to be components of the inflorescence developmental pathway. For example, the region delimited at the top of chromosome 1 harbors *CRY2*, which encodes a blue light receptor protein (Guo *et al.* 1999) and has been shown to affect flowering time in Arabidopsis (Guo *et al.* 1998); *AXR1*, which encodes a protein with similarity to the ubiquitin-activating enzyme E1 (Lincoln *et al.* 1990; Leyser *et al.* 1993); *AXR3*, which encodes a member of the IAA/ARF regulatory gene family (Ouellet *et al.* 2001); and a gene with strong similarity to Zea *DWARF3*, which encodes a cytochrome P450-like enzyme involved in an early step in the GA synthesis pathway (Winkler and Helentjartis 1995; Helliwell *et al.* 2001). Mutations at *AXR1* and *AXR3* affect auxin signaling and result in increased inflorescence branching in Arabidopsis. The region delimited at the top of chromosome 5 harbors flowering-time genes *CONSTANS* (Putterill *et al.* 1995) and *FLC* (Michaels and Amasino 1999), both of which are transcription factors. The region delimited at the bottom of chromosome 5 harbors four genes closely related to *FLC* that are found as tandem duplicates within a 30-kb region (Ratcliffe *et al.* 2001) and a gene in the auxin biosynthetic pathway that encodes ACC synthase.

Collectively, these genes represent plausible candidates that can be pursued through finer-scale mapping efforts and/or complementation tests. It cannot be overemphasized, however, that these remain candidates until definitively shown to be causally associated with *naturally occurring* variation in the observed phenotypes. Indeed, the three chromosomal regions we have focused on (the top of chromosome 1 and the top and bottom of chromosome 5) together contain nearly 1900 discrete genes which, by definition, all hold candidate gene status. More than one-third of these are novel genes of no known function. The previously identified genes described above represent <1% of the total number of genes in these regions.

Resolving a QTL to a single gene remains a formidable task. The genetic tools available in Arabidopsis, however, including the whole genome sequence map, high number of molecular (including single nucleotide polymorphism) markers, availability of mutant lines, and ease of generating T-DNA knockout insertion lines, will undoubtedly facilitate the process. Once QTL can be resolved to a reasonable list of defined candidate genes, quantitative complementation tests (Long *et al.* 1996; Mackay and Fry 1996; Mackay 2001) can be used to define actual genes underlying variation in these traits, providing that suitable mutations in these loci exist and are available in the appropriate genetic backgrounds. Moreover, because Arabidopsis can be readily grown in field conditions, investigators can combine high-resolution genetic information and molecular population genetic analyses with ecological field studies and approach questions about the molecular evolutionary ecology of developmental phenotypes from differing perspectives. The difficulties of these challenges will be offset by the rich genetic information and resulting understanding of naturally occurring variation in development in this model plant species.

The authors thank Johanna Schmitt, Cynthia Weinig, Lisa Dorn, and Carlos Alonso-Blanco for stimulating discussions; and the NCSU Southeastern Plant Environmental Laboratory for use of growth space. This work was supported in part by a National Science Foundation Integrative Research Challenges in Environmental Biology grant to M.D.P., T.F.C.M., and Johanna Schmitt.

LITERATURE CITED

Alonso-Blanco, C., and M. Koornneef, 2000 Naturally occurring variation in *Arabidopsis*: an underexploited resource for plant genetics. Trends Plant Sci. **5:** 22–29.

Alonso-Blanco, C., A. J. M. Peeters, M. Koornneef, C. Lister, C. Dean *et al.*, 1998a Development of an AFLP based linkage map of L*er*, Col and Cvi *Arabidopsis thaliana* ecotypes and construction of a L*er*/Cvi recombinant inbred line population. Plant J. **14:** 259–271.

Alonso-Blanco, C., S. E.-D. El-Assal, G. Coupland and M. Koornneef, 1998b Analysis of natural allelic variation at flowering time loci in the Landsberg *erecta* and Cape Verde Islands ecotypes of *Arabidopsis thaliana*. Genetics **149:** 749–764.

Arabidopsis Genome Initiative, 2000 Analysis of the genome sequence of the flowering plant *Arabidopsis thaliana*. Nature **408:** 796–815.

Basten, C. J., B. S. Weir and Z-B. Zeng, 1994 Zmap—a QTL cartographer, pp. 65–66 in *Proceedings of the 5th World Congress on Genetics Applied to Livestock Production: Computing Strategies and Software*, Vol. 22, edited by C. Smith, J. S. Gavora, B. Benkel, J. Chesnais, W. Fairfull *et al.* The Organizing Committee, 5th World Congress on Genetics Applied to Livestock Production, Guelph, Ontario, Canada.

Basten, C. J., B. S. Weir and Z-B. Zeng, 1999 QTL Cartographer (Version 1.13). Department of Statistics, North Carolina State University, Raleigh, NC.

Blazquez, M., R. Green, O. Nilsson, M. R. Sussman and D. Weigel, 1998 Giberellins promote flowering of *Arabidopsis* by activating the *LEAFY* promoter. Plant Cell **10:** 791–800.

Bowman, J. L., 1994 *Arabidopsis*: *An Atlas of Morphology and Development*. Springer-Verlag, New York.

Bowman, J. L., J. Alvarez, D. Weigel, E. M. Meyerowitz and D. R. Smyth, 1993 Genetic control of flower development in *Arabidopsis thaliana* by *APETALA1* and interacting genes. Development **119:** 721–743.

Bradley, D., O. Ratcliffe, C. Vincent, R. Carpenter and E. Coen, 1997 Inflorescence commitment and architecture in Arabidopsis. Science **275:** 80–83.

Churchill, G. A., and R. W. Doerge, 1994 Empirical threshold values for quantitative trait mapping. Genetics **138:** 963–971.

Clarke, J. H., and C. Dean, 1994 Mapping *FRI*, a locus controlling flowering time and vernalization response in *Arabidopsis thaliana*. Mol. Gen. Genet. **242:** 81–89.

Clarke, J. H., R. Mithen, J. K. M. Brown and C. Dean, 1995 QTL analysis of flowering time in *Arabidopsis thaliana*. Mol. Gen. Genet. **248:** 278–286.

Coen, E. S., and J. M. Nugent, 1994 The evolution of flowers and inflorescences. Development (Suppl.), 107–118.

Diggle, P. K., 1999 Heteroblasty and the evolution of flowering phenologies. Int. J. Plant Sci. **160** (Suppl.): 123–124.

Doerge, R. W., and G. A. Churchill, 1996 Permutation tests for multiple loci affecting a quantitative character. Genetics **142:** 285–294.

Falconer, D. S., and T. F. C. Mackay, 1996 *Introduction to Quantitative Genetics*, Ed. 4. Longman, Essex, UK.

Fishbein, M., and D. L. Venable, 1996 Evolution of inflorescence design: theory and data. Evolution **50:** 2165–2177.

Guo, H. W., W. Y. Yang, T. C. Mockler and C. T. Lin, 1998 Regulation of flowering time by *Arabidopsis* photoreceptors. Science **279:** 1360–1363.

Guo, H. W., H. Duong, N. Ma and C. T. Lin, 1999 The *Arabidopsis* blue light receptor cryptochrome2 is a nuclear protein regulated by a blue light-dependent post-transcriptional mechanism. Plant J. **19:** 279–287.

Helliwell, C. A., P. M. Chandler, A. Poole, E. S. Dennis and W. J. Peacock, 2001 The CTP88A cytochrome P450, ent-kaurenoic acid oxidase, catalyzes three steps of the giberellin biosynthetic pathway. Proc. Natl. Acad. Sci. USA **98:** 2065–2070.

Hempel, F. D., and L. J. Feldmann, 1994 Bidirectional inflorescence development in *Arabidopsis thaliana*. Planta **192:** 276–286.

Houle, D., 1992 Comparing evolvability and variability of quantitative traits. Genetics **130:** 195–204.

Jansen, R. C., J. W. Van Ooijen, P. Stam, C. Lister and C. Dean, 1995 Genotype-by-environment interaction in genetic mapping of multiple quantitative trait loci. Theor. Appl. Genet. **91:** 33–37.

Johanson, U., J. West, C. Lister, S. Michaels, R. Amasino *et al.*, 2000 Molecular analysis of *FRIGIDA*, a major determinant of natural variation in *Arabidopsis* flowering time. Science **290:** 344–347.

Juenger, T., M. Purugganan and T. F. C. Mackay, 2000 Quantitative trait loci for floral morphology in *Arabidopsis thaliana*. Genetics **156:** 1379–1392.

Kempin, S. A., B. Savidge and M. F. Yanofsky, 1995 Molecular basis of the cauliflower phenotype in *Arabidopsis*. Science **267:** 522–525.

Koornneef, M., C. Alonso-Blanco, A. J. M. Peeters and W. Soppe, 1998a Genetic control of flowering time in Arabidopsis. Annu. Rev. Plant Physiol. Plant Mol. Biol. **49:** 345–370.

Koornneef, M., C. Alonso-Blanco, H. Blankestijn-De Vries, C. J. Hanhart and A. J. M. Peeters, 1998b Genetic interactions among late-flowering mutants of Arabidopsis. Genetics **148:** 885–892.

Kosambi, D. D., 1944 The estimation of map distances from recombination values. Ann. Eugen. **12:** 172–175.

Kowalski, S. P., T.-H. Lan, K. A. Feldmann and A. H. Paterson, 1994 QTL mapping of naturally-occurring variation in flowering time of *Arabidopsis thaliana*. Mol. Gen. Genet. **245:** 548–555.

Kuittinen, H., M. J. Sillanpaa and O. Savolainen, 1997 Genetic basis of adaptation: flowering time in *Arabidopsis thaliana*. Theor. Appl. Genet. **95:** 573–583.

Lander, E. S., P. Green, J. Abrahamson, A. Barlow, M. J. Daly *et al.*, 1987 MAPMAKER: an interactive computer package for constructing primary genetic linkage maps of experimental and natural populations. Genomics **1:** 174–181.

Lee, I., M. J. Aukerman, S. L. Gore, K. N. Lohman, S. D. Michaels *et al.*, 1994 Isolation of *LUMINIDEPENDENS*—a gene involved in the control of flowering time in *Arabidopsis*. Plant Cell **6:** 75–83.

Leips, J., and T. F. C. Mackay, 2000 Quantitative trait loci for lifespan in *Drosophila melanogaster*: interactions with genetic background and larval density. Genetics **155:** 1773–1788.

Levy, Y. Y., and C. Dean, 1998 The transition to flowering. Plant Cell **10:** 1973–1989.

Leyser, H. M. O., C. A. Lincoln, C. Timpte, D. Lammer, J. Turner *et al.*, 1993 *Arabidopsis* auxin-resistance gene *AXR1* encodes a protein related to the ubiquitin-activating enzyme E1. Nature **364:** 161–164.

Lincoln, C., J. H. Britton and M. Estelle, 1990 Growth and development of the *AXR1* mutants of *Arabidopsis*. Plant Cell **2:** 1071–1080.

Lister, C., and C. Dean, 1993 Recombinant inbred lines for mapping RFLP and phenotypic markers in *Arabidopsis thaliana*. Plant J. **4:** 745–750.

Long, A. D., S. L. Mullaney, L. A. Reid, J. D. Fry, C. H. Langley *et al.*, 1995 High resolution mapping of genetic factors affecting abdominal bristle number in *Drosophila melanogaster*. Genetics **139:** 1273–1291.

Long, A. D., S. L. Mullaney, T. F. C. Mackay and C. H. Langley, 1996 Genetic interactions between naturally occurring alleles at quantitative trait loci and mutant alleles at candidate loci affecting bristle number in *Drosophila melanogaster*. Genetics **114:** 1497–1510.

Lynch, M., and B. Walsh, 1998 *Genetics and Analysis of Quantitative Traits*. Sinauer Associates, Sunderland, MA.

Mackay, T. F. C., 2001 Quantitative trait loci in *Drosophila*. Nat. Rev. Genet. **2:** 11–20.

Mackay, T. F. C., and J. D. Fry, 1996 Polygenic mutation in *Drosophila melanogaster*: genetic interactions between selection lines and candidate quantitative trait loci. Genetics **144:** 671–688.

Mandel, M. A., C. Gustafson-Brown, B. Savidge and M. F. Yanofsky, 1992 Molecular characterization of the *Arabidopsis* floral homeotic gene *APETALA1*. Nature **360:** 273–277.

Michaels, S. D., and R. M. Amasino, 1999 *FLOWERING LOCUS C* encodes a novel MADS domain protein that acts as a repressor of flowering. Plant Cell **11:** 949–956.

Mitchell-Olds, T., 1996 Genetic contraints on life-history evolution: quantitative-trait loci influencing growth and flowering in *Arabidopsis thaliana*. Evolution **50:** 140–145.

Mitchell-Olds, T., and D. Pedersen, 1998 The molecular basis of quantitative genetic variation in central and secondary metabolism in *Arabidopsis*. Genetics **149:** 739–747.

Napp-Zinn, K., 1969 *Arabidopsis thaliana* (L.) Heynh., pp. 291–304 in *The Induction of Flowering: Some Case Histories*, edited by L. T. Evans. MacMillan, Melbourne.

Napp-Zinn, K., 1985 *Arabidopsis thaliana*, pp. 492–503 in *Handbook of Flowering*, Vol. 1, edited by H. A. Halevy. CRC Press, Boca Raton, FL.

Ouellet, F., P. J. Overvoorde and A. Theologis, 2001 *IAA17/AXR3*: biochemical insight into an auxin mutant phenotype. Plant Cell **13:** 829–841.

Putterill, J., F. Robson, K. Lee, R. Simon and G. Coupland, 1995 The *CONSTANS* gene of *Arabidopsis* promotes flowering and encodes a protein showing similarities to zinc-finger transcription factors. Cell **80:** 847–857.

Rieseberg, L. H., M. A. Archer and R. K. Wayne, 1999 Transgressive segregation, adaptation and speciation. Heredity **83:** 363–372.

Roberston, A., 1959 The sampling variance of the genetic correlation coefficient. Biometrics **15:** 469–485.

Sanda, S., M. John and R. Amasino, 1997 Analysis of flowering time in ecotypes of *Arabidopsis thaliana*. J. Hered. **88:** 69–72.

SAS Institute, 1988 *SAS/STAT User's Guide, Release 6.03 Edition*. SAS Institute, Cary, NC.

SAS Institute, 1999 *Statview Reference Manual*. SAS Institute, Cary, NC.

Schmitz, G., and K. Theres, 1999 Genetic control of branching in Arabidopsis thaliana. Curr. Opin. Plant Biol. **2:** 51–55.

Schoen, D. J., and M. Dubec, 1990 The evolution of inflorescence size and number—a gamete-packaging strategy in plants. Am. Nat. **135:** 841–857.

Shannon, S., and D. R. Meeks-Wagner, 1991 A mutation in the *Arabidopsis TFL1* gene affects inflorescence meristem development. Plant Cell **3:** 877–892.

Shannon, S., and D. R. Meeks-Wagner, 1993 Genetic interactions that regulate inflorescence development in Arabidopsis. Plant Cell **5:** 639–655.

Sheldon, C. C., J. E. Burn, P. P. Perez, J. Metzger, J. A. Edwards *et al.*, 1999 The *FLF* MADS box gene: a repressor of flowering in *Arabidopsis* regulated by vernalization and methylation. Plant Cell **11:** 445–458.

Simpson, G. G., A. R. Gendall and C. Dean, 1999 When to switch to flowering. Annu. Rev. Cell Dev. Biol. **15:** 519–531.

Sokal, R. R., and F. J. Rohlf, 1995 *Biometry: The Principles and Practice of Statistics in Biological Research*, Ed. 3. W. H. Freeman and Company, New York.

Stratton, D. A., 1998 Reaction norm functions and QTL-environment interactions for flowering time in *Arabidopsis thaliana*. Heredity **81:** 144–155.

Suarez-Lopez, P., K. Wheatley, F. Robson, H. Onouchi, F. Valverde *et al.*, 2001 *CONSTANS* mediates between the circadian clock and the control of flowering time in *Arabidopsis*. Nature **410:** 1116–1120.

Sussex, I. M., and N. M. Kerk, 2001 The evolution of plant architecture. Curr. Opin. Plant Biol. **4:** 33–37.

Swarup, K., C. Alonso-Blanco, J. R. Lynn, S. D. Michaels, R. M. Amasino *et al.*, 1999 Natural allelic variation identifies new genes in the *Arabidopsis* circadian system. Plant J. **20:** 67–77.

Tanksley, S. D., 1993 Mapping polygenes. Annu. Rev. Genet. **27:** 205–233.

Tucker, S. C., and J. Grimes, 1999 The inflorescence. Bot. Rev. **65:** 303–316.

Wade, M. J., 1992 Sewall Wright: gene interaction and the shifting balance theory. Oxf. Surv. Evol. Biol. **8:** 35–62.

Walker, L., and M. Estelle, 1998 Molecular mechanisms of auxin action. Curr. Opin. Plant Biol. **1:** 434–439.

Weigel, D., J. Alvarez, D. R. Smyth, M. F. Yanofsky and E. M. Meyerowitz, 1992 *LEAFY* controls floral meristem identity in *Arabidopsis*. Cell **69:** 843–859.

Winkler, R. G., and T. Helentjaris, 1995 The maize *DWARF3* gene encodes a cytochrome P450-mediated early step in giberellin biosynthesis. Plant Cell **7:** 1307–1317.

Yano, M., 2001 Genetic and molecular dissection of naturally occurring variation. Curr. Opin. Plant Biol. **4:** 130–135.

Zeng, Z-B., 1993 Theoretical basis of separation of multiple linked gene effects on mapping quantitative trait loci. Proc. Natl. Acad. Sci. USA **90:** 10972–10976.

Zeng, Z-B., 1994 Precision mapping of quantitative trait loci. Genetics **136:** 1457–1468.

Communicating editor: O. Savolainen